Journal of
Medicinal Chemistry

Article

Discovery of Novel Aryl Carboxamide Derivatives as Hypoxia-inducible Factor (HIF) 1# Signaling Inhibitors with Potent Activities of Anticancer Metastasis

Mingming Liu, Yuru Liang, Zhongzhen Zhu, Jin Wang, Xingxing Cheng, Jiayi Cheng, Binpeng Xu, Rong Li, XinHua Liu, and Yang Wang

J. Med. Chem., **Just Accepted Manuscript** • DOI: 10.1021/acs.jmedchem.9b01313 • Publication Date (Web): 26 Sep 2019

is published by the American Chemical Society. 1155 Sixteenth Street N.W., Washington, DC 20036

Discovery of Novel Aryl Carboxamide Derivatives as Hypoxia-inducible Factor (HIF) 1α Signaling Inhibitors with Potent Activities of Anticancer Metastasis

Mingming Liu[1,3,4,#], Yuru Liang[2,#], Zhongzhen Zhu[1,#], Jin Wang[1], Xingxing Cheng[1], Jiayi Cheng[2], Binpeng Xu[4], Rong Li[1], Xinhua Liu[1,] and Yang Wang[2,*]*

1. School of Pharmacy, Anhui Medical University, Hefei 230032, China
2. School of Pharmacy, Fudan University, Shanghai 201203, China
3. Shanghai Key Laboratory of New Drug Design, East China University of Science and Technology, Shanghai 200237, China
4. Anhui Chem-Bright Bioengineering Co., Ltd., Huaibei 235025, China

Abstract

In order to discover novel HIF-1 inhibitors for cancer metastasis treatment, 68 new aryl carboxamide compounds were synthesized and evaluated for their inhibitory effect by dual luciferase-reporter assay. Based on five rounds of investigation on structure-activity relationships (SARs) step by step, compound **30m** was discovered as the most active inhibitor (IC_{50}=0.32 μM) with no obvious cytotoxicity (CC_{50}>50 μM). It effectively attenuated hypoxia-induced HIF-1α protein accumulation and reduced transcription of VEGF in a dose-dependent manner, which was further demonstrated by its inhibitory potency on capillary-like tube formation, angiogenesis of zebrafish as well as cellular migration and invasion. Importantly, compound **30m** exhibited anti-metastatic potency in breast cancer lung metastasis in mice model, indicating its promising therapeutic potential for prevention and treatment of tumor metastasis. These results definitely merit attention for further rational design of more efficient HIF-1 inhibitors in the future.

1. Introduction

Cancer metastasis is a multiple process in which cancer cells disseminate from the primary tumor to distant secondary organs through the circulatory system. The migratory and invasive capabilities facilitate metastatic cells to invade through basement membrane, intravasate into Lumina or blood vessels, and extravasate into the parenchyma of distant tissues, thereby generating clinically detectable metastatic tumors[1-2]. Metastasis remains the leading cause of therapeutic failure and responsible for over 90% of cancer-associated patient mortality, mainly due to the reason that most of the current chemotherapeutic agents control tumor growth rather than its metastasis.[3-4] Recent advance in the understanding of the molecular signaling pathway that regulates metastatic spread provides potential therapeutic targets for cancer metastasis prevention and inhibition.[5-6]

Hypoxia-inducible factor 1 (HIF-1), a transcription factor that responds to a hypoxic environment, is a heterodimer composed of HIF-1α and HIF-1β subunits. Under normoxia condition, the hydroxylated HIF-1α subunit is recognized by the von Hippel–Lindau (VHL) E3-ubiquitin ligase complex, and subjected to proteasomal degradation subsequently[7-8]. Whereas, under hypoxic conditions, the absence of oxygen and decreasing hydroxylation stabilize HIF-1α, resulting in its nuclear translocation and dimerization with HIF-1β. The heterodimer binds to the hypoxia responsive element (HRE) located in the region of target genes promotor, and therefore activates transcription of a number of downstream target genes.[9-10] These genes encode proteins, including vascular epidermal growth factor (VEGF), matrix metalloproteases (MMPs), snail1, twist and glucose transporter type 1 (GLUT1), et al.,[11-15] which promote cancer development and metastasis through enhancing cellular motility and invasiveness, inducing epithelial-mesenchymal transition (EMT) and cancer stem cell properties, promoting angiogenesis, reprogramming glucose metabolism, and resisting apoptosis.[16-19] Recent studies have highlighted that dramatic overexpression of HIF-1 was measured in many human cancers, such as breast cancer,

ovarian cancer, hepatocellular carcinoma, cervical cancer and so on, leading to tumor metastasis and poor patient prognosis.[20-22] Therefore, HIF-l has been considered to be a promising target for the development of novel therapeutics against cancer metastasis.[23-25]

In recent years, a number of small-molecule inhibitors have been identified with the capacity to reduce the transcriptional activities of HIF-1 or to induce HIF-1α degradation (**Figure 1**), including adamantyl-based inhibitors (**1**, LW6), carborane-based inhibitors (**2**, GN26361,), manassantin A (**3**) and derivatives, deguelin (**4**) and its ring-truncated derivatives (**5**, SH-1280), sulfonamide derivatives (**6**, KCN), YC-1 (**7**) and derivatives etc.[26-33] Most of these inhibitors were discovered through high throughput screening (HTS) or natural products screening with large molecular weight, complicated chemical structures, relative hydrophobicity, poor water solubility and low potency, which thereby limited their further development. Unfortunately, there is no HIF-1 inhibitor ~~has been~~ approved by FDA for cancer treatment up to date. Therefore, there is still an urgent need to discover novel HIF-1 inhibitors with sufficient potency, low toxicity, good druggability and novel chemical diversity.

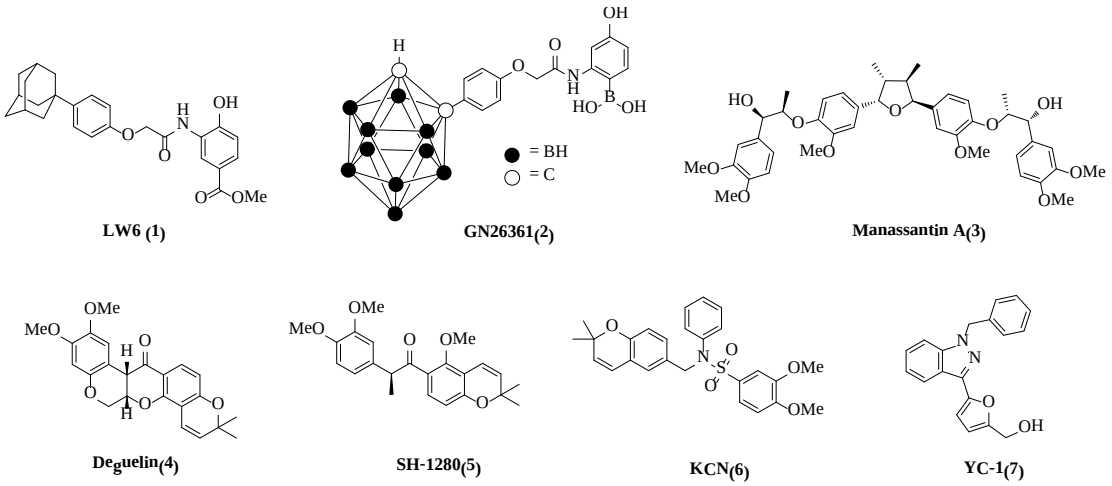

Figure 1. Structures of representative HIF-1α inhibitors.

Considering the advantages of fragment-based approaches in discovering novel leading compounds, an in-house fragments collection (M.W. < 300 Da) was screened

using HRE luciferase reporter assay to identify hits of HIF-1 inhibitors for further optimization. From the screening, a thiazole carboxamide fragment **8** (M.W. = 246 Da, **Figure 2**) was identified as a preliminary hit containing moderate inhibitory effect with the IC_{50} value of 55.7 μM. Biological evaluation showed that this hit inhibited the invasion and migration of breast cancer MDA-MB-231 cells without obvious cytotoxicity. These results encouraged us to conduct further structural optimization and structure-activity relationships (SARs) studies to improve the potency for intervention of cancer metastasis. Therefore, based on the chemical structure of this hit and rational drug design, a small-molecular library of 68 novel aryl carboxamide derivatives was constructed and evaluated as HIF-1 inhibitors.

2. Design

In order to carry out more extensive rational design, the modification and SAR study of hit **8** were approached in a step-by-step manner. As shown in **Figure 2**, the hit was divided into three regions, namely the methyl group (region **A**), the thiazole ring (region **B**) and the phenyl group (region **C**) by the connection of *N*-ethyl amide (**Linker**). Firstly, region **C** was modified with several substituted phenyl and heterocyclic groups as well as the length of **Linker** was investigated, resulting in 2-chlorophenyl and 4-pyridyl analogs with improved activities (**step 1**). For fragment growing, phenyl or heterocycles were introduced to replace the methyl group (region **A**). The results from SAR showed that introduction of phenyl into region **A** achieved increasing activities (**step 2**). Next, the thiazole ring (region **B**) was replaced with a variety of five- and six-membered aromatic rings, including pyridine-2-carbonamide which showed relatively better activity (**step 3**). Then, the substituent on the phenyl ring of region **C** was further optimized, and the replacement of chlorine with fluorine dramatically increased activity (**step 4**). Finally, the phenyl group of region **A** was replaced with a variety of heterocycles and substituted phenyl, and 2-methoxyl phenyl substituent turned out to be the best alternative with activity of almost 170-fold stronger than that of hit **8** (**step 5**).

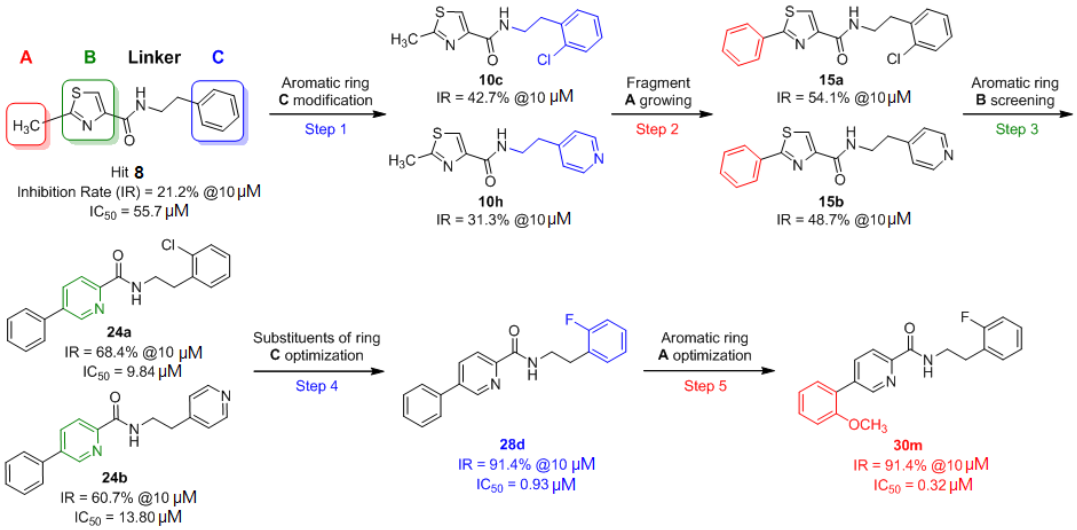

Figure 2. Structural optimization step by step.

3. Chemistry

As depicted in **Scheme 1**, thiazole and other aryl carboxamides (**8**, **10a-h**,**12a-f)** were prepared by acylation of various substituted amines with corresponding aryl carbonyl chlorides, which were generated by the reaction of commercial available acids (**9** and **11a-c)** with oxalyl chloride.

Scheme 1. Synthesis of 8, 10a-h and 12a-f

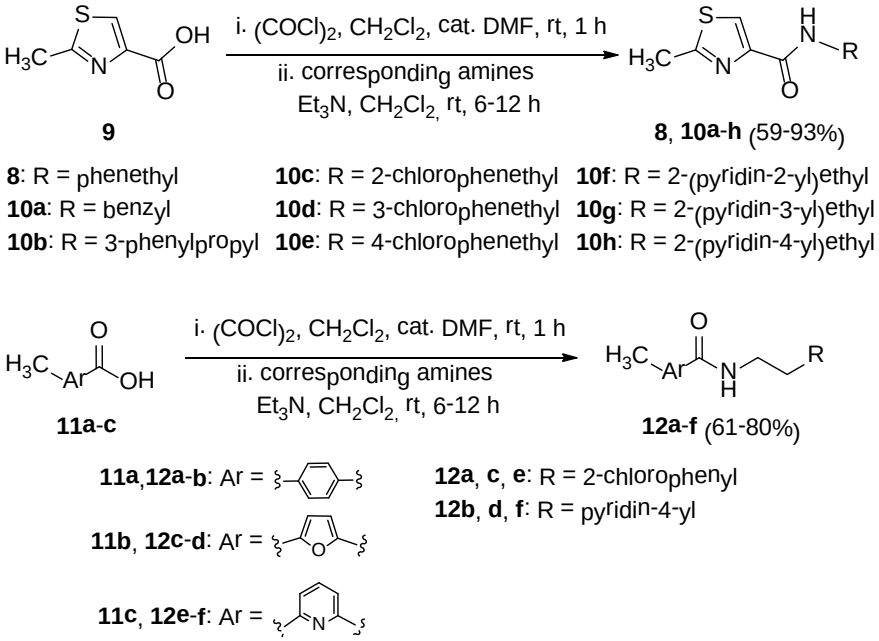

The synthesis of five-membered heterocycles carboxamides **15a-f** and **18a-j** was

described in **Scheme 2**. As key intermediate, aryl thiazolyl carboxylic acid ethyl esters (**13a-c**), phenyl oxazolyl carboxylic acid ethyl esters (**16a-b**), and phenyl oxadiazolyl carboxylic acid ethyl esters (**16c-e**) were synthesis according to the literatures[34-35], respectively (see supporting information). Hydrolysis of the esters **13a-c** and **16a-e** with LiOH in ethanol produced the corresponding acids **14a-c** and **17a-e**, respectively. Finally, the targeted thiazole, oxazole and oxadiazole carboxamides **15a-f** and **18a-j** were obtained by a similar procedure described in **Scheme 1**.

Scheme 2. Synthesis of 15a-f and 18a-j

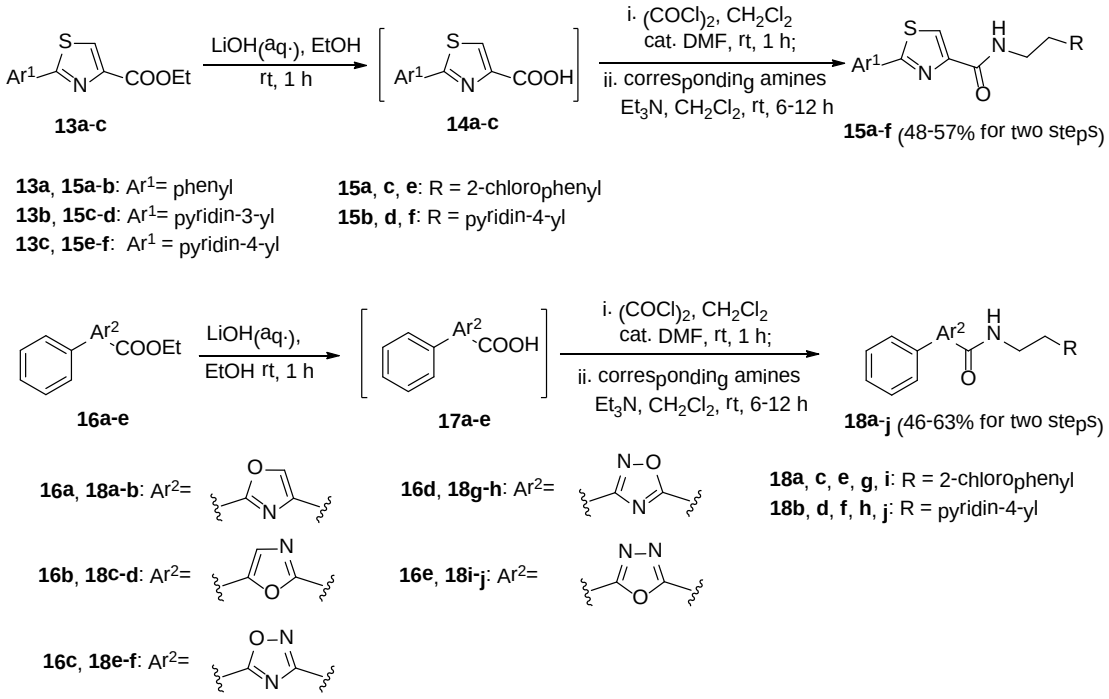

As outlined in **Scheme 3**, Suzuki coupling of phenylboronic acid (**21**) with 5-bromopicolinic acid (**22a**) or 6-bromonicotinic acid (**22b**) in the presence of $Pd(PPh_3)_2Cl_2$ afforded phenyl substituted pyridine carboxylic acids **23a-b**. pyrimidine-4-carboxamide **25a** and pyrimidine-2-carboxamide **25b** were synthesized according to the literature[36] (see supporting information) and were then hydrolyzed in 20% H_2SO_4 (aq.) to give the corresponding pyrimidine carboxylic acids **26a-b**, respectively. Finally, the targeted amides **20a-b**, **24a-d**, and **27a-b** were obtained by a similar procedure described in **Scheme 1**.

Scheme 3. Synthesis of 20a-b, 24a-d, and 27a-b.

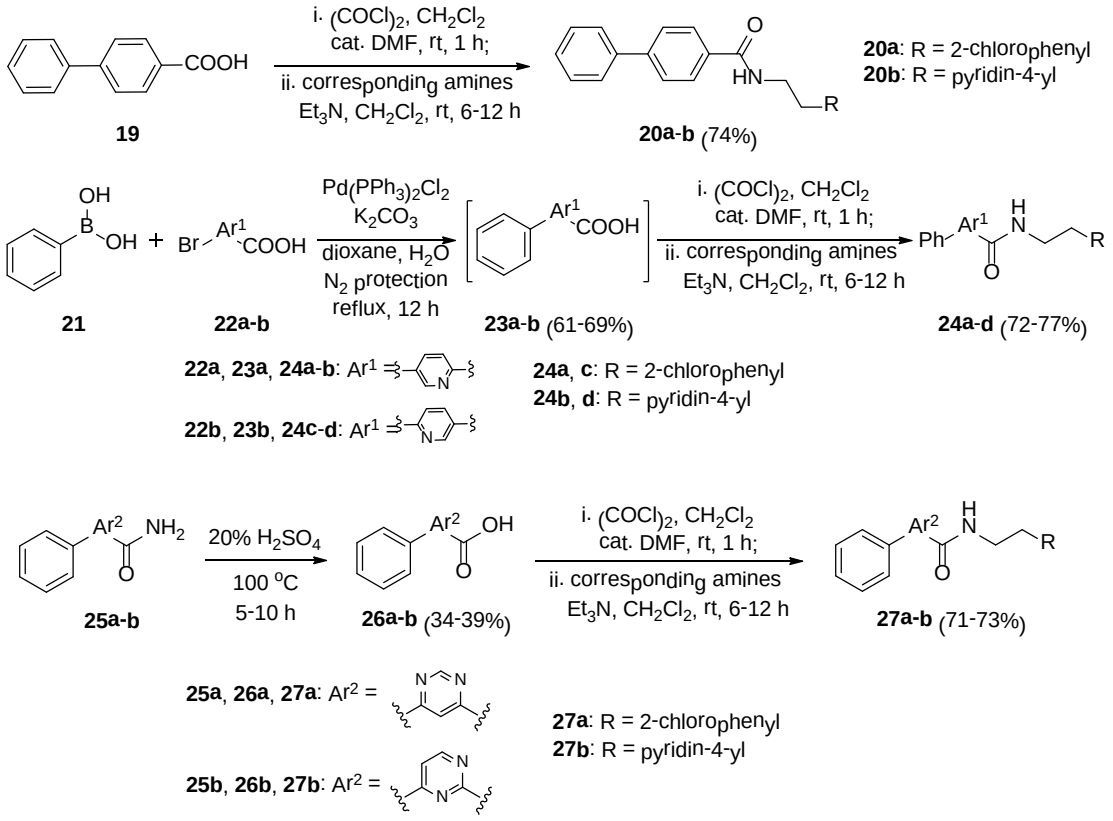

As described in **Scheme 4**, the synthesis of series of 5-phenylpicolinic amides **28a-l** was similar to that of compounds **20a-b**. Meanwhile, acylation of 2-fluorophenethylamine by 5-bromopicolinic acid (**22a**), followed by Suzuki coupling reaction with various aryl boronic acids, gave the target 5-aryl substituted picolinic amides **30a-r**.

Scheme 4. Synthesis of 28a-l and 30a-r

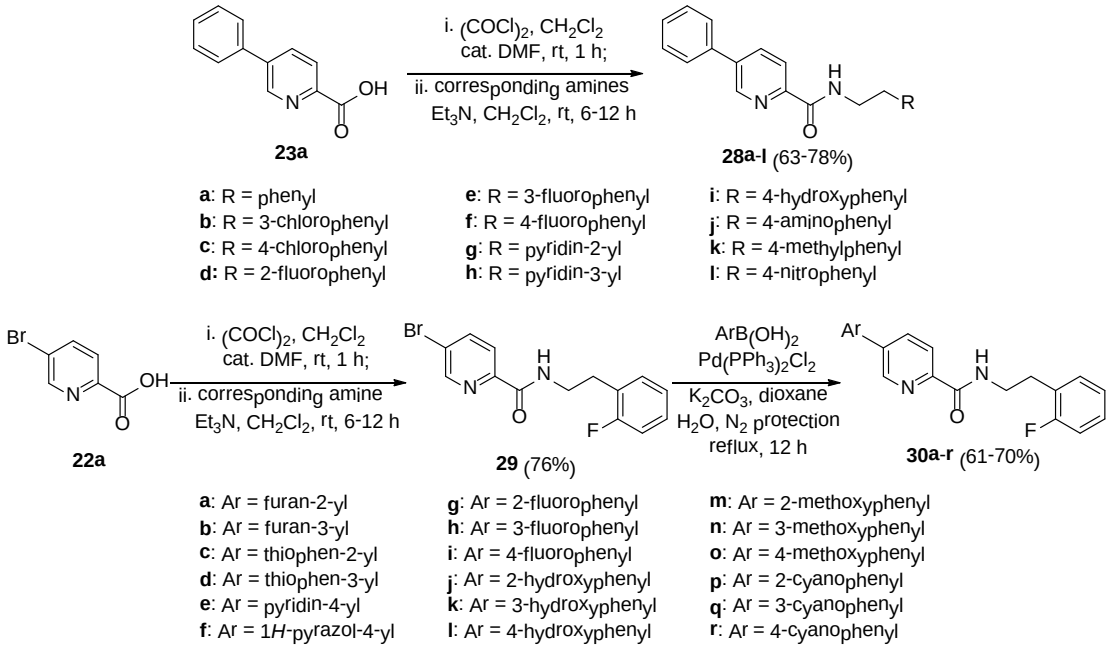

3. RESULT AND DISCUSSION

3.1 Cell-based HRE Assay and SAR Studies.

To improve the potency of hit **8** and identify more effective inhibitors of HIF-1, 68 new compounds were designed and synthesized based on SAR studies step by step. The inhibition rates (IR) of synthesized compounds were initially determined at 10 μM by HRE luciferase reporter assay in human hepatocellular carcinoma LM3 cells under hypoxia condition. In the assay, LM3 cells were co-transfected with a HIF-1 reporter vector which contains five copies of HRE sequences located in the region of firefly luciferase gene promotor along with pRL-SV40 plasmid encoding Renilla luciferase. After transfection, cells were treated with tested compounds and incubated under hypoxia. Under hypoxic condition, accumulated heterodimers of HIF-1α and HIF-1β bound to the HRE sequences and prompted the transcription of firefly luciferase. Inhibition of HIF-1 signaling by tested compounds reduced the expression of firefly luciferase leading to diminish the firefly luminescence. To determine the inhibitory effect of synthesized compounds, firefly luminescence signal was measured by using a microplate reader and normalized to the luminescence of Renilla luciferase. LW6 (**1**) was selected as positive control.[37]

Firstly, we examined the effect of the phenethyl group (region **C** and Linker) of hit

8 on inhibitory activity. As listed in **Table 1**, replacement of phenethyl by benzyl (**10a**) or 3-phenylpropyl (**10b**) decreases the potency, indicating that favorable length of two C atoms between N and phenyl. Introduction of a chlorine atom at ortho- position of the phenyl ring (**10c**) significantly increased the potency, whereas meta- or para-substitution diminished it. Replacement of phenyl by pyridin-4-yl (**10h**) led to increasing IR from 21.2% to 31.3%. Based on this findings, 2-chlorophenethyl and 2-(pyridin-4-yl)ethyl were fixed in the following structural optimization (**Figure 2**).

Table 1. HIF-1 Inhibition Activities of Hit 8 and Compounds 10a-h at 10 μM

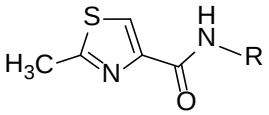

Compound	R	HRE Inhibition (%) ± SD
8	phenethyl	21.2 ± 3.1
10a	benzyl	3.1 ± 2.4
10b	3-phenylpropyl	6.5 ± 0.3
10c	2-chlorophenethyl	42.7 ± 6.6
10d	3-chlorophenethyl	1.2 ± 1.1
10e	4-chlorophenethyl	0.6 ± 1.1
10f	2-(pyridin-2-yl)ethyl	5.1 ± 2.7
10g	2-(pyridin-3-yl)ethyl	2.4 ± 1.9
10h	2-(pyridin-4-yl)ethyl	31.3 ± 5.2
1 (LW6)		73.5 ± 4.7

As listed in **Table 2**, keeping the 2-chlorophenethyl or 2-(pyridin-4-yl)ethyl unchanged, thiazole ring (region **B**) was replaced by other aromatic rings, such as phenyl (**12a-b**), furan (**12c-d**) and pyridine (**12e-f**), resulting in no obvious improvement of activities. Replacing methyl group (region **A**) with phenyl ring led to increasing potency as shown by compounds **15a-b**, however, introduction of pyridin-3-yl (**15c-d**) or pyridin-4-yl (**15e-f**) appeared to be unfavorable. Therefore, we fixed phenyl ring as region **A** and focused on the modification of thiazole ring

(**Figure 2**).

Table 2. HIF-1 Inhibition Activities of Compounds 12a-f and 15a-f at 10 μM

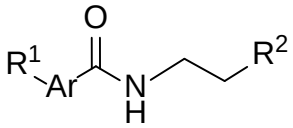

Compound	R^1	Ar	R^2	HRE Inhibition (%) ± SD
12a	Me	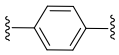	2-chlorophenyl	45.3 ± 3.2
12b	Me	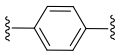	pyridin-4-yl	3.1 ± 5.1
12c	Me	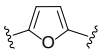	2-chlorophenyl	17.4 ± 14.3
12d	Me	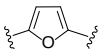	pyridin-4-yl	12.8 ± 4.0
12e	Me	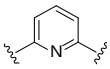	2-chlorophenyl	37.3 ± 9.2
12f	Me	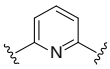	pyridin-4-yl	36.4 ± 5.1
15a	phenyl	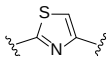	2-chlorophenyl	54.1 ± 6.6
15b	phenyl	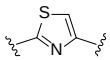	pyridin-4-yl	48.7 ± 7.4
15c	pyridin-3-yl	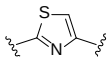	2-chlorophenyl	21.6 ± 3.4
15d	pyridin-3-yl	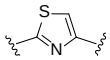	pyridin-4-yl	33.9 ± 7.8
15e	pyridin-4-yl	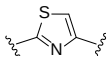	2-chlorophenyl	18.4 ± 2.1
15f	pyridin-4-yl	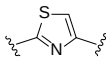	pyridin-4-yl	19.9 ± 3.5

To explore the influence of aromatic ring of region **B** against HIF-1 inhibitory activity, a variety of five- and six-membered aromatic rings were screened. As listed in **Table 3**, all of these phenyl substituted aromatic carboxamides showed moderate to potent inhibitory activities with IR values ranging from 36.9-77.2%, indicating the critical role of phenyl substitution of region **A**. In general, six-membered aromatic ring derivatives (**20a-b**, **24a-d**, and **27a-b**) exhibited more effective inhibition than

five-membered heterocyclic ones (**18a-j**), possibly due to their appropriate ring size or polarities for the binding site. More interestingly, *N*-2-chlorophenethyl substituted biphenyl carboxamide (**20a**) showed the highest potency (IR = 77.2%), which may imply that the aromatic ring in region **C** mainly exerts π-π stacking or hydrophobic interaction instead of hydrogen-bond effects, whereas the corresponding *N*-2-(pyridin-4-yl)ethyl substituent (**20b**) displayed reduced inhibitory activity (IR = 42.0%). Considering that both picolinamides (**24a-b**) possessed acceptable potency, with IR values of 68.4% and 60.7%, respectively, we next fixed 5-phenylpicolinamide group to region **B** and further modified the substitution on phenyl group in region **C** (**Figure 2**).

Table 3. HIF-1 Inhibition Activities of Compounds 18a-j, 20a-b, 24a-d, and 27a-b at 10 μM

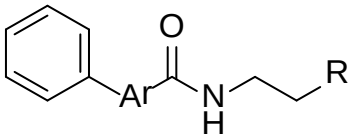

Compound	Ar	R	HRE Inhibition (%) ± SD
18a	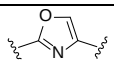	2-chlorophenyl	51.4 ± 6.4
18b	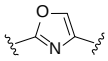	pyridin-4-yl	38.7 ± 3.8
18c	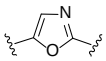	2-chlorophenyl	52.3 ± 2.2
18d	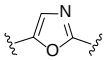	pyridin-4-yl	53.5 ± 1.7
18e	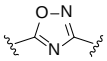	2-chlorophenyl	40.5 ± 6.4
18f	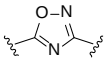	pyridin-4-yl	49.7 ± 4.8
18g	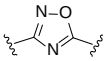	2-chlorophenyl	44.1 ± 9.0
18h	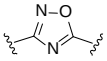	pyridin-4-yl	36.9 ± 7.2
18i	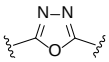	2-chlorophenyl	41.8 ± 2.9
18j	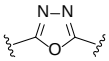	pyridin-4-yl	67.3 ± 1.2

20a	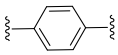	2-chlorophenyl	77.2 ± 4.8
20b	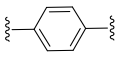	pyridin-4-yl	42.0 ± 5.5
24a	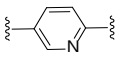	2-chlorophenyl	68.4 ± 5.6
24b	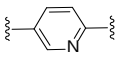	pyridin-4-yl	60.7 ± 6.4
24c	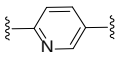	2-chlorophenyl	45.1 ± 2.8
24d	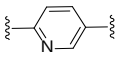	pyridin-4-yl	47.4 ± 2.6
27a	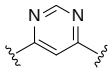	2-chlorophenyl	56.7 ± 4.9
27b	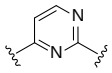	pyridin-4-yl	61.5 ± 3.4

Compared with **24a**, unexpectedly, deletion of the chlorine atom of region **C** (**28a**) significantly elevated the inhibitory activity (**Table 4**) with IR values increasing from 68.4% to 82.2%, suggesting no obvious correlation between the electronic effects of substituent and activities. Subsequently, we examined the positional effect of the chlorine and fluorine on the phenyl ring. It turned out that most of chlorine and fluorine substitution (**28b-c** and **28e-f**) showed weaker activities than that of unsubstituted derivative (**28a**), except the *ortho*-fluorine substituted derivative (**28d**) with IR value of 91.4%. In addition, pyridin-2-yl, pyridin-3-yl and para-hydroxyl, amino, methyl, nitro substituted phenyl derivatives (**28g-l**) displayed unsatisfied activities.

Table 4. HIF-1 Inhibition Activities of Compounds 28a-l at 10 μM

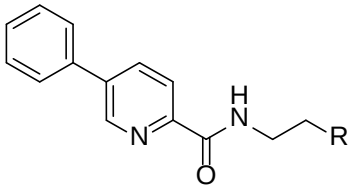

Compound	R	HRE Inhibition (%) ± SD
28a	phenyl	82.2 ± 4.1
28b	3-chlorophenyl	64.6 ± 5.7

28c	4-chlorophenyl	58.2 ± 8.3
28d	2-fluorophenyl	91.4 ± 4.4
28e	3-fluorophenyl	58.7 ± 2.6
28f	4-fluorophenyl	46.1 ± 11.2
28g	pyridin-2-yl	43.7 ± 7.9
28h	pyridin-3-yl	44.5 ± 0.9
28i	4-hydroxyphenyl	36.9 ± 4.1
28j	4-aminophenyl	60.2 ± 3.7
28k	4-methylphenyl	31.8 ± 3.0
28l	4-nitrophenyl	40.2 ± 2.8

On the basis of SAR studies above, we maintained *N*-(2-fluorophenethyl)picolinamide and optimized the phenyl ring of region **A** (**Figure 2**). As listed in **Table 5**, eighteen compounds were designed, synthesized and evaluated for HIF-1 inhibition. Among them, thiophen-3-yl substituted compound (**30d**) maintained HIF-1 inhibitory potency similar with that of **28d**, while furanyl, pyridinyl and pyrazolyl substitutions (**30a-b**, and **30e-f**) resulted in decreased activities more or less. In regard to substituted phenyl derivatives (**30g-r**), *ortho*-substitutions were more favorable than *meta*- and *para*-substitutions; fluorine (**30g-i**) and methoxy (**30m-o**) substitutions displayed acceptable activities. Particularly, 2-methoxyphenyl derivative (**30m**) was the most active inhibitor with IR value of 97.7%.

Table 5. HIF-1 Inhibition Activities of Compounds 30a-r at 10 μM

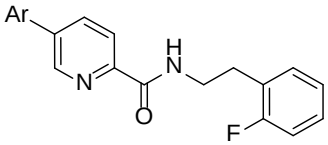

Compound	Ar	HRE Inhibition (%) ± SD
30a	furan-2-yl	57.2 ± 7.7
30b	furan-3-yl	73.4 ± 6.1

30c	thiophen-2-yl	80.0 ± 2.0
30d	thiophen-3-yl	88.2 ± 3.5
30e	pyridin-4-yl	57.5 ± 3.1
30f	1*H*-pyrazol-4-yl	29.5 ± 4.1
30g	2-fluorophenyl	83.8 ± 9.4
30h	3-fluorophenyl	55.3 ± 14.2
30i	4-fluorophenyl	41.2 ± 12.4
30j	2-hydroxyphenyl	43.6 ± 5.0
30k	3-hydroxyphenyl	0.3 ± 1.5
30l	4-hydroxyphenyl	33.2 ± 4.1
30m	2-methoxyphenyl	97.7 ± 1.4
30n	3-methoxyphenyl	53.8 ± 3.8
30o	4-methoxyphenyl	45.6 ± 6.4
30p	2-cyanophenyl	62.7 ± 2.7
30q	3-cyanophenyl	44.5 ± 7.1
30r	4-cyanophenyl	13.1 ± 6.9

Finally, fifteen compounds with IR more than 60% were selected for determination of their IC_{50} values (**Table 6**). Among them, 6 compounds with IC_{50} values below 3 μM, showed better HIF-1 inhibitory activity than that of positive control **1**, and no obvious cytotoxicity was observed (CC_{50} > 50 μM). To summarize, of these 68 newly synthesized compounds, **30m** was the most active compound with an IC_{50} value of 0.32 μM, almost 10-fold more effective than that of **1**.[37] In comparison to the structure of original hit **8**, the 2-methoxyphenyl group (region **A**) is essential for the activity, the replacement of thiazole by pyridine (region **B**) improves the potency, and the introduction of fluorine atom to the phenyl ring (region **C**) is beneficial to the inhibitory effect. Thus, through five rounds of optimization, **30m** showed over 170-fold enhancement of inhibitory activity against HIF-1 compared with the hit **8** and therefore was selected for further bioactivity evaluation.

Table 6. IC_{50} Values of Selected Compounds against HIF-1

Compound	HRE IC_{50} (μM)	Cytotoxicity CC_{50} (μM)
18j	7.32	>50
20a	2.87	>50
24a	9.84	>50
24b	13.80	>50
27b	10.04	>50
28a	4.56	>50
28b	9.84	>50
28d	0.93	>50
28j	11.61	>50
30b	4.24	>50
30c	2.48	>50
30d	1.41	>50
30g	2.16	>50
30m	0.32	>50
30p	8.53	>50
1 (LW6)	3.08	>50

3.2 Inhibition of HIF-1α Accumulation

To further confirm their inhibition of HIF-1 pathway, representative compounds **30f**, **30b** and **30m** with low, moderate and high potency in HRE reporter assay, respectively, hit **8**, as well as **1** as positive control were evaluated for inhibition of HIF-1α protein accumulation under hypoxia condition using western blot assay. As shown in **Figure 3A**, the effects of the tested compounds on HIF-1α protein accumulation were consistent with their potency in HRE luciferase reporter assay. Among the selected compounds, compound **30m** showed the most activity against HIF-1α accumulation, even stronger than the positive control **1**. Accordingly, the inhibitory effects of **30m** on HIF-1α accumulation were also evaluated in other cancer cell lines including breast cancer (MDA-MB-231), ovarian cancer (SKOV3) and cervical cancer (HeLa). As expected, **30m** attenuated HIF-1α accumulation in a

dose-dependent manner in all of the tested cell lines (**Figure 3B**). Our recent results from qRT-PCR of HIF-1α mRNA and HIF-1α protein degradation assay indicated that **30m** probably prompted the degradation of HIF-1α protein (data not shown). Next, we plan to synthesize the biotin-based photo-cross-linking probe of **30m** and to conduct affinity pull-down experiment in order to identify the direct target of **30m**. Taken together, our data preliminarily indicated that compound **30m** could block the HIF pathway by reduction of HIF-1α protein level and prompted us to further evaluate the effects of this compound on angiogenesis and tumor cellular metastasis.

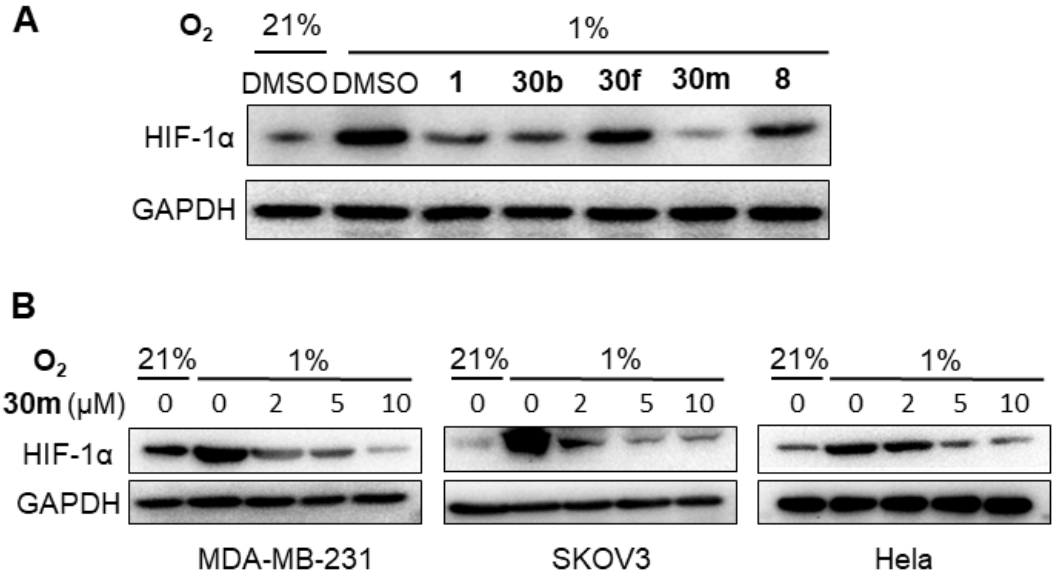

Figure 3. Effects of selected compounds on hypoxia-induced accumulation of HIF-1α. (**A**) The expression of HIF-1α was examined in LM3 cells treated with selected compounds, including compounds **30b**, **30f**, **30m** and **8** at the concentration of 10 μM under hypoxia. **1** (LW6) was used as positive control. (**B**) The effects of compound **30m** on hypoxia-induced HIF-1α accumulation were determined in various human cancer cell lines, including MDA-MB-231, SKOV3, and HeLa at indicated concentrations.

3.3 Inhibition of Compound 50m on Angiogenesis

VEGF, the target gene directly regulated by HIF-1, promotes hypoxia-induced angiogenesis, which is essential for cancer progression and metastasis.[11-12] Silencing

HIF-1/VEGF pathway, which results in reduced ability of malignant cells to recruit vasculature and colonize at distant sites, has emerged as promising strategy for cancer treatment.[19] Accordingly, we firstly determined effects of compound **30m** on transcription of VEGF in human umbilical vein endothelial cells (HUVECs). Results obtained from real-time assay showed that **30m** effectively reduced the mRNA levels of VEGF in a dose-dependent manner (**Figure 4A**). Next, capillary-like tube formation assay was performed to further evaluate the anti-angiogenesis activity of compound **30m** *in vitro*. As shown in **Figure 4B**, hypoxia induced a complete network structure formed by HUVECs, whereas treatment with **30m** significantly suppressed the tubule formation at non-antiproliferative concentrations (2 and 5 μM). Particularly, at concentration of 5 μM, **30m** completely disrupted the formation of tube structures. Furthermore, the *in vivo* anti-angiogenic activity of **30m** was further determined by transgenic zebrafish, in which the vascular endothelial cells were labeled with green fluorescent protein (GFP). Zebrafish embryos were selected, dechlorinated, and incubated with 0.5 or 1 μM of **30m** for 24 h, meanwhile 0.5 μM of commercial VEGFR inhibitor apatinib served as a positive control. The affection of zebrafish subintestinal vessels (SIVs) was observed under a fluorescence microscope. **Figure 4C** illustrated the obvious destruction of zebrafish SIVs by exposure to compound **30m**, indicating that **30m** effectively blocked the growth of normal angiogenesis with similar activities of the positive control apatinib (**Figure 4D**).

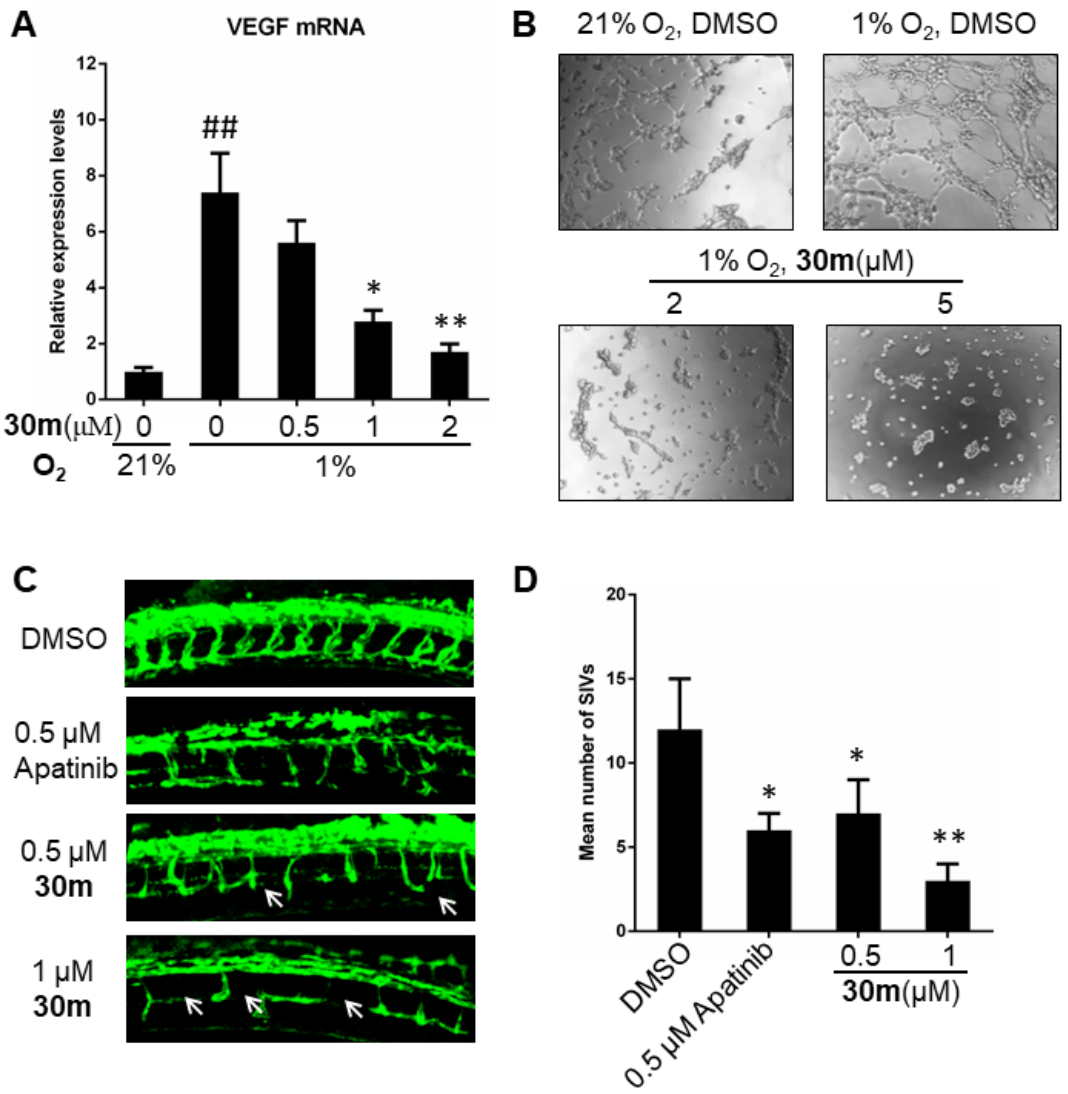

Figure 4. Effects of compound **30m** on angiogenesis *in vitro* and *in vivo*. (**A**) Relative expression of VEGF mRNA was determined by real-time PCR after treatment of HUVECs with 0.5 or 1 μM of compound **30m**. Relative expression of VEGF was normalized against GAPDH. Results represent the means ± SD from three independent experiments. $^{\#\#}p<0.01$ vs normoxia group; $^{*}p<0.05$, $^{**}p<0.01$ *vs* untreated control. (**B**) Inhibition of hypoxia-induced capillary-like tube formation. HUVECs were seeded in the 96-well plate pre-coated with matrigel, and incubated with 2 or 5 μM of compound **30m**. Tubule branches were photographed. A representative result from three independent experiments is shown. (**C**) Inhibitory effect of compound **30m** on the angiogenesis of transgenic zebrafish. Zebrafish was

treated with **30m** (0.5 and 1 μM) or DMSO (n = 10), and the subintestinal vessels (SIVs) of zebrafish were observed using confocal microscopy. Apatinib was used as a positive control. Representative images from three independent experiments were shown. White arrows indicated the destruction of SIVs. (**D**) Histogram showed the numbers of zebrafish SIVs per field under confocal microscopy. Results represented the means ± SD. *p<0.05, **p<0.01 *vs* untreated control.

3.4 Inhibition of Compound 30m on Cellular Migration and Invasion

Increased evidence indicates that, through HIF-1 activation, hypoxia stimulates the expression of certain genes promoting tumor cellular invasiveness and metastasis, such as MMPs and EMT regulators.[13-14, 18-19] Therefore, we performed wound healing and transwell assays to examine the inhibitory effects of compound **30m** on migration and invasion of breast cancer MDA-MB-231 cells under hypoxic condition. To avoid induction of apoptosis or growth arrest, cells were treated with non-toxic concentrations (2, 5 and 10 μM) of **30m** for 24 h. Results from wound healing assay showed that **30m** dose-dependently impaired the ability of cells to close a wound**,** indicating the inhibition of cellular migration *in vitro* (**Figure 5A**). In transwell assay, MDA-MB-231 cells were seeded into upper chambers with or without pre-coated matrigel stimulating base-membrane for determination of cellular invasion or migration, respectively. As illustrated in **Figure 5B** and **5C**, the numbers of both migratory and invasive cells were significantly reduced by **30m** in a dose-dependent manner. Furthermore, western blot assay was used to investigate whether compound **30m** could affect the expression of HIF-1 downstream genes related to cancer metastasis. As shown in **Figure 5D**, treatment of **30m** dose-dependently induced E-cadherin expression but repressed vimentin expression in MDA-MB-231 cells, indicating the reversal of hypoxia-mediated EMT process. In addition, western blot analysis also showed that **30m** dose-dependently down-regulated the expression of MMP-2 and MMP-9, which mediate extracellular matrix (ECM) degradation and thereby promotes cancer metastasis. Together, these results implied that compound

30m inhibited migration and invasion of cancer cells with inhibition of EMT process and down-regulation of MMPs.

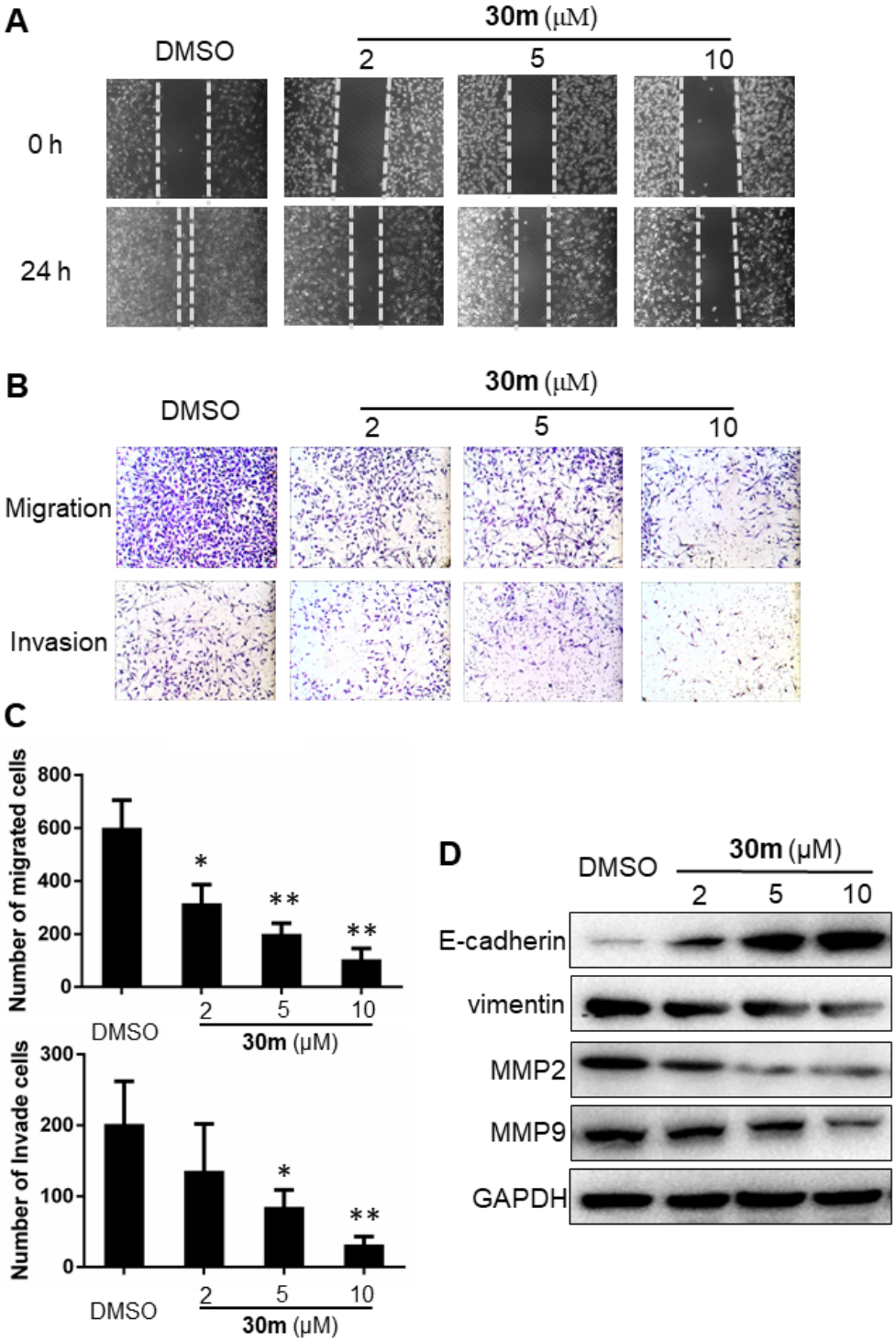

Figure 5. Effects of compound **30m** on cellular migration and invasion. (**A**) Inhibition of cellular migration by compound **30m** in wound-healing assay. After a single wound was scratched on cellular monolayer, MDA-MB-231 cells were treated with

compound **30m** (2, 5 and 10 μM) or DMSO under normoxia for 1 h and hypoxia for another 24 h. Representative images from three independent experiments were shown. (**B**) Inhibition of cellular migration and invasion by compound **30m** in transwell assays. MDA-MB-231 cells were seeded on chambers with or without pre-coated matrigel for invasion or migration assay, respectively. After incubated with compound **30m**, cells that migrated through the chambers were stained with crystal violet. Representative images from three independent experiments were shown. (**C**) Histogram shows the numbers of migrated and invasive cells. The experiments were repeated three times and results were indicated as means ± SD. *p<0.05, **p<0.01 *vs* untreated control. (**D**) The expression of E-cadherin, Vimentin, MMP-2 and MMP-9 were determined by western blotting assay. GAPDH was selected as loading control. Representative results from three independent experiments were shown.

4.5 Inhibition of Compound 30m on Tumor Metastasis *In Vivo*

With great interests to discover anti-metastatic agents, we evaluated the inhibitory potency of compound **30m** using breast cancer lung metastasis mice model, which was established by intravenous injection of MDA-MB-231 cells stable expressing luciferase. Mice were treated with **30m** or vehicle intraperitoneally (i.p.) every 2 days during 3 weeks. After the final administration, bioluminescent imaging techniques were used to assess the ability of malignant cells to generate lung metastases. After the mice were sacrificed, the lung metastatic nodules were examined by histology. Results obtained from quantitative analysis of bioluminescent signal (**Figure 6A** and **6B**) and hematoxylin and eosin (H&E) staining (**Figure 6D**) revealed that treatment with compound **30m** significantly reduced lung colonization of tumor cells in dose-dependent manner without obvious body-weight loss (**Figure 6C**). These results indicated the therapeutic effects and low toxicity of compound **30m** in metastatic breast cancer mice model.

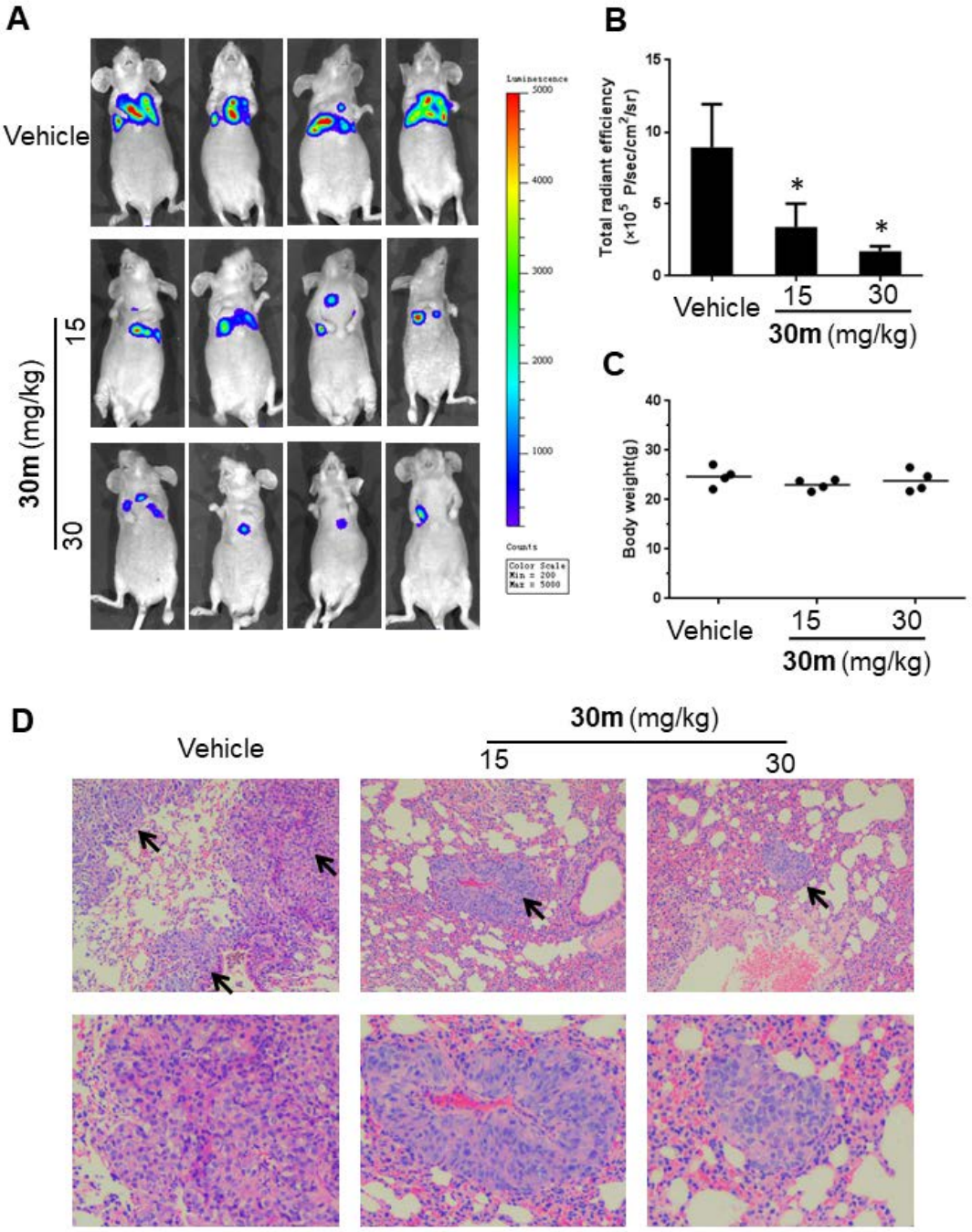

Figure 6. Compound **30m** inhibited the formation of metastasis of human breast cancer cells in mice model. (**A**) MDA-MB-231 cells stably transfected with luciferase were injected directly into the tail vein of BALB/c nude mice. Mice then received vehicle or compound **30m** (15 and 30 mg/kg) starting 24 h after injection of cells. Animals received therapy every 2 days during 20 days. Bioluminescent images were acquired 24 h after the final dose of inhibitor. (**B**) Quantification of bioluminescence.

Data are expressed as the mean ± SD (n = 4 per group) *p<0.05. (**C**) The body weights of the mice recorded at the end of the experiment. (**D**) Photomicrographs of mice lung tissue sections stained with H&E illustrated the formation of breast cancer metastasis. Black arrows indicated the metastatic nodules of breast cancer.

4. CONCLUSION

In the present study, in order to discover novel therapeutics for cancer metastasis, series of aryl carboxamide derivatives were synthesized and evaluated for inhibition of HIF-1 signaling pathway by dual luciferase-reporter assay. Starting from the fragment hit 2-methyl-N-phenethylthiazole-4-carboxamide (**8)**, systematic lead optimization was carried out, in an attempt to improve potency. In particular, replacement of methyl with 2-methoxyl substituted phenyl, conversion of the thiazole moiety to pyrimidine moiety and introduction of F atom to the phenyl ring of *N*-phenethyl led to increasing the HIF-1 inhibitory activities. After five rounds of in-depth study on SAR step by step, compound **30m** was discovered as the most active inhibitor (IC_{50} = 0.32 μM) without obvious cytotoxicity (CC_{50} > 50 μM). Further biological evaluation showed that it could dose-dependently block hypoxia-induced HIF-1α protein accumulation in several human cancer cell lines. Besides, it down-regulated transcription of VEGF, a downstream gene of HIF-1, which was consistent with its inhibitory potency on capillary-like tube formation *in vitro* and angiogenesis of zebrafish *in vivo*. Moreover, compound **30m** inhibited migration and invasion of tumor cells *in vitro* and blocked breast cancer lung metastasis in mice model, indicating the promising therapeutic potential of compound **30m** as an effective HIF-1 inhibitor to prevent tumor metastasis and progression. Therefore, the above results are of great importance in the development of more efficient HIF-1 inhibitors for cancer therapy.

5. EXPERIMENTAL SECTION

5.1 Chemistry

All commercial reagents and solvents were purchased from commercial suppliers and used without further purification. Reactions were monitored by thin-layer chromatography (TLC) and visualized under UV light at 254 and 365 nm. The chromatograms were conducted on silica gel (300-400 mesh) using combiflash chromatography systems (Teledyne ISCO Rf200). ^{1}H and ^{13}C NMR spectral data were recorded with a Bruker 600 MHz spectrometer in $CDCl_3$ or DMSO-d_6 using tetramethylsilane (TMS) as the internal standard. High-resolution mass spectrometry (HRMS) was recorded on an Agilent Technologies LC-TOF instrument. Targeted compounds were analyzed by a Shimadzu LC20A HPLC instrument with a UV/visible detector (5 μm, 4.6 mm×150 mm C_{18} column). The purities of all targeted compounds were determined by monitoring at 254 nm and were confirmed to be more than 95% (Table S1).

General procedure for the synthesis of compounds 8, 10a-h, 12a-f, 15a-f, 18a-j, 20a-b, 24a-d, 27a-b, 28a-l, and 29 exemplified by 2-methyl-*N*-phenethylthiazole-4-carboxamide (8). To a solution of 2-methylthiazole-4-carboxylic acid (143 mg, 1 mmol) in dry CH_2Cl_2 (5 mL), oxalyl chloride (0.17 mL) and DMF (1 drop) were added at 0 °C. Then, the resulting mixture was stirred at room temperature for 1 h and concentrated in vacuo to give the 2-methylthiazole-4-carbonyl chloride as crude product. To a solution of 2-phenylethanamine (121 mg, 1 mmol) in CH_2Cl_2 (5 mL) was added Et_3N (0.16 mL) and the 2-methylthiazole-4-carbonyl chloride redissolved in CH_2Cl_2 (1 mL). The reaction mixture was stirred at room temperature for additional 6-12 h. The solution was concentrated in vacuo. The residue was purified by flash chromatography to yield compound **8** as a white solid (216 mg, 93%). ^{1}H NMR (600 MHz, $CDCl_3$) δ 7.93 (s, 1H), 7.40 (brs, 1H), 7.33-7.30 (m, 2H), 7.25-7.22 (m, 3H), 3.69 (q, J = 6.0 Hz, 2H), 2.93 (t, J = 6.0 Hz, 2H), 2.68 (s, 3H); ^{13}C NMR (151 MHz, $CDCl_3$) δ 165.26, 160.52, 149.12, 138.31, 128.16, 127.98, 125.84, 122.17, 40.02, 35.35, 18.46; ESI-HRMS (*m/z*) calcd $C_{13}H_{14}N_2OS$ (M + H^+) 247.0900, found 247.0899.

***N*-Benzyl-2-methylthiazole-4-carboxamide (10a).** White solid, yield 73%. ^{1}H NMR (600 MHz, $CDCl_3$) δ 7.97 (s, 1H), 7.62 (brs, 1H), 7.36-7.32 (m, 4H), 7.29-7.26

(m, 1H), 4.63 (d, J = 6.0 Hz, 2H), 2.67 (s, 3H); ^{13}C NMR (151 MHz, $CDCl_3$) δ 165.36, 160.42, 148.95, 137.57, 128.07, 127.28, 126.86, 122.48, 42.75, 18.43; ESI-HRMS (*m/z*) calcd $C_{12}H_{12}N_2OS$ (M + H^+) 233.0743, found 233.0741.

2-Methyl-*N*-(3-phenylpropyl)thiazole-4-carboxamide (10b). Colorless oil, yield 64%. ^{1}H NMR (600 MHz, $CDCl_3$) δ 7.93 (s, 1H), 7.36 (brs, 1H), 7.29-7.26 (m, 2H), 7.20-7.17 (m, 3H), 3.48-3.45 (m, 2H), 2.72-2.71 (m, 2H), 2.69 (s, 3H), 1.97-1.92 (m, 2H); ^{13}C NMR (151 MHz, $CDCl_3$) δ 165.82, 161.12, 149.82, 141.40, 128.39, 128.35, 125.91, 122.65, 38.89, 33.24, 31.25, 19.05; ESI-HRMS (*m/z*) calcd $C_{14}H_{16}N_2OS$ (M + H^+) 261.1056, found 261.1059.

***N*-(2-Chlorophenethyl)-2-methylthiazole-4-carboxamide (10c).** Colorless oil, yield 84%. ^{1}H NMR (600 MHz, $CDCl_3$) δ 7.94 (s, 1H), 7.42 (brs, 1H), 7.36 (dd, J = 7.4, 1.4 Hz, 1H), 7.28-7.26 (m, 1H), 7.20-7.17 (m, 2H), 3.70 (q, J = 7.4 Hz, 2H), 3.06 (t, J = 7.4 Hz, 2H), 2.68 (s, 3H); ^{13}C NMR (151 MHz, $CDCl_3$) δ 165.85, 161.17, 149.70, 136.52, 134.15, 130.92, 129.57, 127.97, 126.92, 122.77, 38.97, 33.66, 19.04; ESI-HRMS (*m/z*) calcd $C_{13}H_{13}ClN_2OS$ (M + H^+) 281.0510, found 281.0512.

***N*-(3-Chlorophenethyl)-2-methylthiazole-4-carboxamide (10d).** White solid, yield 59%. ^{1}H NMR (600 MHz, $CDCl_3$) δ 7.94 (s, 1H), 7.37 (brs, 1H), 7.24-7.21 (m, 3H), 7.13-7.12 (m, 1H), 3.67 (q, J = 7.3 Hz, 2H), 2.90 (t, J = 7.3 Hz, 2H), 2.69 (s, 3H); ^{13}C NMR (151 MHz, $CDCl_3$) δ 165.39, 160.56, 148.92, 140.32, 133.71, 129.25, 128.34, 126.37, 126.10, 122.31, 39.74, 35.03, 18.48; ESI-HRMS (*m/z*) calcd $C_{13}H_{13}ClN_2OS$ (M + H^+) 281.0510, found 281.0513.

***N*-(4-Chlorophenethyl)-2-methylthiazole-4-carboxamide (10e).** White solid, yield 70%. ^{1}H NMR (600 MHz, $CDCl_3$) δ 7.93 (s, 1H), 7.37 (brs, 1H), 7.28-7.27 (m, 2H), 7.18-7.16 (m, 2H), 3.66 (q, J = 7.2 Hz, 2H), 2.90 (t, J = 7.2 Hz, 2H), 2.68 (s, 3H); ^{13}C NMR (151 MHz, $CDCl_3$) δ 165.38, 160.54, 148.94, 136.75, 131.66, 129.52, 128.09, 122.30, 39.85, 34.69, 18.50; ESI-HRMS (*m/z*) calcd $C_{13}H_{13}ClN_2OS$ (M + H^+) 281.0510, found 281.0510.

2-Methyl-*N*-(2-(pyridin-2-yl)ethyl)thiazole-4-carboxamide (10f). Colorless oil, yield 72%. ^{1}H NMR (600 MHz, $CDCl_3$) δ 8.57 (d, J = 4.7 Hz, 1H), 7.92 (s, 1H), 7.86 (brs, 1H), 7.62-7.59 (m, 1H), 7.20 (d, J = 7.8 Hz, 1H), 7.16-7.14 (m, 1H), 3.85 (q, J =

6.7 Hz, 2H), 3.10 (t, *J* = 6.7 Hz, 2H), 2.68 (s, 3H); ^{13}C NMR (151 MHz, $CDCl_3$) δ 165.77, 161.13, 159.29, 149.88, 149.35, 136.45, 123.31, 122.62, 121.47, 38.65, 37.50, 19.08; ESI-HRMS (*m/z*) calcd $C_{12}H_{13}N_3OS$ (M + H^+) 248.0852, found 248.0849.

2-Methyl-*N*-(2-(pyridin-3-yl)ethyl)thiazole-4-carboxamide (10g). White solid, yield 85%. ^{1}H NMR (600 MHz, $CDCl_3$) δ 8.49 (d, *J* = 1.6 Hz, 1H), 8.48 (dd, *J* = 4.8, 1.6 Hz, 1H), 7.92 (s, 1H), 7.57 (dt, *J* = 7.8, 1.6Hz, 1H), 7.41 (brs, 1H), 7.24 (dd, *J* = 7.8, 4.8 Hz, 1H), 3.69 (q, *J* = 7.0 Hz, 2H), 2.94 (t, *J* = 7.0 Hz, 2H), 2.67 (s, 3H); ^{13}C NMR (151 MHz, $CDCl_3$) δ 165.41, 160.60, 149.56, 148.84, 147.43, 135.61, 133.70, 122.88, 122.36, 39.62, 32.52, 18.45; ESI-HRMS (*m/z*) calcd $C_{12}H_{13}N_3OS$ (M + H^+) 248.0852, found 248.0856.

2-Methyl-*N*-(2-(pyridin-4-yl)ethyl)thiazole-4-carboxamide (10h). White solid, yield 77%. ^{1}H NMR (600 MHz, $CDCl_3$) δ 8.52 (d, *J* = 5.8 Hz, 2H), 7.93 (s, 1H), 7.38 (brs, 1H), 7.17 (d, *J* = 5.8 Hz, 2H), 3.71 (q, *J* = 7.2 Hz, 2H), 2.93 (t, *J* = 7.2 Hz, 2H), 2.67 (s, 3H); ^{13}C NMR (151 MHz, $CDCl_3$) δ 165.45, 160.59, 149.33, 148.78, 147.27, 123.51, 122.41, 38.89, 34.63, 18.45; ESI-HRMS (*m/z*) calcd $C_{12}H_{13}N_3OS$ (M + H^+) 248.0852, found 248.0855.

***N*-(2-Chlorophenethyl)-4-methylbenzamide (12a).** White solid, yield 80%. ^{1}H NMR (600 MHz, $CDCl_3$) δ 7.62-7.60 (m, 2H), 7.38-7.37 (m, 1H), 7.27-7.26 (m, 1H), 7.22-7.17 (m, 4H), 6.17 (brs, 1H), 3.73 (q, *J* = 6.8 Hz, 2H), 3.09 (t, *J* = 6.8 Hz, 2H), 2.38 (s, 3H); ^{13}C NMR (151 MHz, $CDCl_3$) δ 166.87, 141.20, 136.08, 133.51, 131.10, 130.50, 129.05, 128.59, 127.48, 126.42, 126.19, 39.09, 32.73, 20.79; ESI-HRMS (*m/z*) calcd $C_{16}H_{16}ClNO$ (M + H^+) 274.0993, found 274.0993.

4-Methyl-*N*-(2-(pyridin-4-yl)ethyl)benzamide (12b). White solid, yield 80%. ^{1}H NMR (600 MHz,$CDCl_3$) δ 8.50 (d, *J* = 5.7 Hz, 2H), 7.60 (d, *J* = 7.8 Hz, 2H), 7.20 (d, *J* = 7.8 Hz, 2H), 7.15 (d, *J* = 5.7 Hz, 2H), 6.28 (brs, 1H), 3.71 (q, *J* = 7.0 Hz, 2H), 2.93 (t, *J* = 7.0 Hz, 2H), 2.38 (s, 3H); ^{13}C NMR (151 MHz, $CDCl_3$) δ 167.00, 149.26, 147.58, 141.43, 130.83, 128.63, 126.24, 123.62, 39.65, 34.51, 20.82; ESI-HRMS (*m/z*) calcd $C_{15}H_{16}N_2O$ (M + H^+) 241.1335, found 241.1337.

***N*-(2-Chlorophenethyl)-5-methylfuran-2-carboxamide (12c).** Colorless oil, yield 67%. ^{1}H NMR (600 MHz, $CDCl_3$) δ 7.37 (dd, *J* = 7.5, 1.5 Hz, 1H), 7.28-7.26 (m,

1H), 7.22-7.17 (m, 2H), 6.99 (d, *J* = 3.3 Hz, 1H), 6.37 (brs, 1H), 6.08 (d, *J* = 3.3 Hz, 1H), 3.68 (td, *J* = 7.0 Hz, 2H), 3.05 (t, *J* = 7.0 Hz, 2H), 2.32 (s, 3H); ^{13}C NMR (151 MHz, $CDCl_3$) δ 158.59, 154.32, 146.38, 136.51, 134.13, 131.00, 129.59, 128.02, 126.96, 115.28, 108.43, 38.77, 33.62, 13.74; ESI-HRMS (*m/z*) calcd $C_{14}H_{14}ClNO_2$ (M + H^+) 264.0786, found 264.0789.

5-Methyl-*N*-(2-(pyridin-4-yl)ethyl)furan-2-carboxamide (12d). White solid, yield 70%. ^{1}H NMR (600 MHz, $CDCl_3$) δ 8.51 (d, *J* = 5.8, 2H), 7.15 (d, *J* = 5.8 Hz, 2H), 6.99 (d, *J* = 3.3 Hz, 1H), 6.43 (brs, 1H), 6.07 (d, *J* = 3.3, 1H), 3.68 (q, *J* = 7.0 Hz, 2H), 2.91 (t, *J* = 7.0 Hz, 2H), 2.29 (s, 3H); ^{13}C NMR (151 MHz, $CDCl_3$) δ 158.00, 153.94, 149.31, 147.32, 145.50, 123.56, 114.99, 107.95, 38.68, 34.67, 13.18; ESI-HRMS (*m/z*) calcd $C_{13}H_{14}N_2O_2$ (M + H^+) 231.1128, found 231.1128.

***N*-(2-Chlorophenethyl)-6-methylpicolinamide (12e).** Colorless oil, yield 61%. ^{1}H NMR (600 MHz, $CDCl_3$) δ 8.23 (brs, 1H), 7.99 (d, *J* = 7.7 Hz, 1H), 7.71 (t, *J* = 7.7 Hz, 1H), 7.37 (dd, *J* = 7.5, 1.5 Hz, 1H), 7.29 (d, *J* = 7.5 Hz, 1H), 7.27-7.25 (m, 1H), 7.22-7.16 (m, 2H), 3.74 (q, *J* = 7.1 Hz, 2H), 3.09 (t, *J* = 7.1 Hz, 2H), 2.54 (s, 3H); ^{13}C NMR (151 MHz, $CDCl_3$) δ 164.56, 157.05, 149.21, 137.38, 136.66, 134.18, 130.99, 129.57, 127.95, 126.89, 125.74, 119.14, 39.05, 33.63, 24.17; ESI-HRMS (*m/z*) calcd $C_{15}H_{15}ClN_2O$ (M + H^+) 275.0946, found 275.0949.

6-Methyl-*N*-(2-(pyridin-4-yl)ethyl)picolinamide (12f). Colorless oil, yield 73%. ^{1}H NMR (600 MHz, $CDCl_3$) δ 8.53 (d, *J* = 5.9 Hz, 2H), 8.25-8.15 (m, 1H), 7.98 (d, *J* = 7.7 Hz, 1H), 7.72 (t, *J* = 7.7 Hz, 1H), 7.27 (d, *J* = 7.7 Hz, 1H), 7.19 (d, *J* = 5.9 Hz, 2H), 3.74 (q, *J* = 7.0 Hz, 2H), 2.96 (t, *J* = 7.0 Hz, 2H), 2.53 (s, 3H); ^{13}C NMR (151 MHz, $CDCl_3$) δ 164.59, 157.13, 149.93, 148.97, 147.96, 137.46, 125.91, 124.13, 119.19, 39.58, 35.30, 24.18; ESI-HRMS (*m/z*) calcd $C_{14}H_{15}N_3O$ (M + H^+) 242.1288, found 242.1289.

General procedure for the synthesis of compounds 14a-c and 17a-e exemplified by 2-phenylthiazole-4-carboxylic acid (14a). 2*N* LiOH aqueous solution was added to a solution of carboxylic ester **13a** (1 eq) in ethanol at ambient temperature. The reaction mixture was stirred for 1 h, and ethanol was then removed by evaporation in vacuo. The resulting mixture was adjusted to pH = 5-6 with 1*N* HCl.

The precipitated white solid was collected by filtration and dried to give the carboxylic acid **14a** as a white solid (68% yield), which was used in next step without further purification.

***N*-(2-Chlorophenethyl)-2-phenylthiazole-4-carboxamide (15a).** White solid, yield 48% from **9a**. ^{1}H NMR (600 MHz, $CDCl_3$) δ 8.09 (s, 1H), 7.94-7.92 (m, 2H), 7.59 (brs, 1H), 7.47-7.46 (m, 3H), 7.39 (dd, *J* = 7.4, 1.7 Hz, 1H), 7.31 (dd, *J* = 7.4, 1.7 Hz, 1H), 7.24-7.19 (m, 2H), 3.76 (q, J = 7.0 Hz, 2H), 3.12 (t, *J* = 7.0 Hz, 2H); ^{13}C NMR (151 MHz, $CDCl_3$) δ 167.46, 160.57, 150.19, 135.94, 133.59, 132.25, 130.45, 129.99, 129.04, 128.44, 127.46, 126.37, 125.99, 122.14, 38.47, 32.99; ESI-HRMS (*m/z*) calcd $C_{18}H_{15}ClN_2OS$ (M + H^+) 349.0714, found 349.0702.

2-Phenyl-*N*-(2-(pyridin-4-yl)ethyl)thiazole-4-carboxamide (15b). White solid, yield 49% from **9a**. ^{1}H NMR (600 MHz, $CDCl_3$) δ 8.56 (d, *J* = 5.8 Hz, 2H), 8.09 (s, 1H), 7.92-7.90 (m, 2H), 7.56 (brs, 1H), 7.47-7.46 (m, 3H), 7.23 (d, *J* = 5.8 Hz, 2H), 3.77 (q, *J* = 7.2 Hz, 2H), 2.99 (t, *J* = 7.2 Hz, 2H); ^{13}C NMR (151 MHz, $CDCl_3$) δ 167.65, 160.57, 149.91, 149.39, 147.25, 132.13, 130.09, 128.47, 125.96, 123.56, 122.38, 38.99, 34.72; ESI-HRMS (*m/z*) calcd $C_{17}H_{15}N_3OS$ (M + H^+) 332.0828, found 332.0831.

***N*-(2-Chlorophenethyl)-2-(pyridin-3-yl)thiazole-4-carboxamide (15c).** White solid, yield 53% from **9b**. ^{1}H NMR (600 MHz, $CDCl_3$) δ 9.16 (s, 1H), 8.70 (d, *J* = 5.4 Hz, 1H), 8.19 (d, *J* = 7.8 Hz, 1H), 8.15 (s, 1H), 7.42-7.38 (m, 2H), 7.30 (d, *J* = 7.8 Hz, 1H), 7.24-7.19 (m, 2H), 3.77 (t, *J* = 7.0 Hz, 2H), 3.12 (t, *J* = 7.0 Hz, 2H); ^{13}C NMR (151 MHz, $CDCl_3$) δ 164.08, 160.22, 150.72, 150.65, 147.08, 135.84, 133.59, 133.11, 130.43, 129.08, 128.26, 127.55, 126.39, 123.16, 122.88, 38.54, 32.90; ESI-HRMS (*m/z*) calcd $C_{17}H_{14}ClN_3OS$ (M + H^+) 344.0619, found 344.0618.

2-(Pyridin-3-yl)-*N*-(2-(pyridin-4-yl)ethyl)thiazole-4-carboxamide (15d). White solid, yield 51% from **9b**. ^{1}H NMR (600 MHz, $CDCl_3$) δ 9.13 (d, *J* = 1.5 Hz, 1H), 8.68 (dd, *J* = 4.8, 1.5 Hz, 1H), 8.54 (d, *J* = 6.0 Hz, 2H), 8.20-8.18 (m, 1H), 8.19 (s, 1H), 7.53 (brs, 1H), 7.40 (dd, *J* = 8.0, 4.8 Hz, 1H), 7.19 (d, *J* = 6.0 Hz, 2H), 3.76 (q, *J* = 7.2 Hz, 2H), 2.98 (t, *J* = 7.2 Hz, 2H); ^{13}C NMR (151 MHz, $CDCl_3$) δ 164.27, 160.24, 150.81, 150.39, 149.40, 147.15, 147.06, 133.08, 128.16, 123.53, 123.19,

123.13, 39.04, 34.65; ESI-HRMS (*m/z*) calcd $C_{16}H_{14}N_4OS$ (M + H^+) 311.0961, found 311.0966.

***N*-(2-Chlorophenethyl)-2-(pyridin-4-yl)thiazole-4-carboxamide (15e).** White solid, yield 57% from **9c**. ^{1}H NMR (600 MHz, $CDCl_3$) δ 8.74 (dd, *J* = 4.6, 1.5 Hz, 2H), 8.21 (s, 1H), 7.78 (dd, *J* = 4.6, 1.5 Hz, 2H), 7.39 (dd, *J* = 7.3, 1.7 Hz, 1H), 7.30 (dd, *J* = 7.1, 1.9 Hz, 1H), 7.24-7.19 (m, 2H), 3.76 (t, *J* = 7.2 Hz, 2H), 3.12 (t, *J* = 7.2 Hz, 2H); ^{13}C NMR (151 MHz, $CDCl_3$) δ 164.54, 160.02, 150.90, 150.19, 138.89, 135.82, 133.59, 130.43, 129.08, 127.55, 126.40, 123.80, 119.68, 38.46, 32.88; ESI-HRMS (*m/z*) calcd $C_{17}H_{14}ClN_3OS$ (M + H^+) 344.0619, found 344.0619.

2-(Pyridin-4-yl)-*N*-(2-(pyridin-4-yl)ethyl)thiazole-4-carboxamide (15f). White solid, yield 56% from **9c**. ^{1}H NMR (600 MHz, $CDCl_3$) δ 8.73 (d, *J* = 6.0 Hz, 2H), 8.54 (d, *J* = 5.8 Hz, 2H), 8.21 (s, 1H), 7.75 (d, *J* = 6.0 Hz, 2H), 7.49 (brs, 1H), 7.19 (d, *J* = 5.8 Hz, 2H), 3.77 (q, *J* = 7.2 Hz, 2H), 2.98 (t, *J* = 7.2 Hz, 2H); ^{13}C NMR (151 MHz, $CDCl_3$) δ 164.74, 160.09, 150.65, 150.23, 149.41, 147.11, 138.76, 124.03, 123.54, 119.64, 39.05, 34.65; ESI-HRMS (*m/z*) calcd $C_{16}H_{14}N_4OS$ (M + H^+) 311.0961, found 311.0965.

***N*-(2-Chlorophenethyl)-2-phenyloxazole-4-carboxamide (18a).** White solid, yield 48% from **16a**. ^{1}H NMR (600 MHz, $CDCl_3$) δ 8.23 (s, 1H), 8.03-8.02 (m, 2H), 7.50-7.47 (m, 3H), 7.39 (dd, *J* = 7.5, 1.5 Hz, 1H), 7.30 (dd, *J* = 7.3, 1.7 Hz, 1H), 7.24-7.18 (m, 2H), 7.16 (brs, 1H), 3.73 (q, *J* = 7.2 Hz, 2H), 3.10 (t, *J* = 7.2 Hz, 2H); ^{13}C NMR (151 MHz, $CDCl_3$) δ 161.37, 160.74, 140.69, 137.26, 136.41, 134.17, 131.00, 130.98, 129.62, 128.87, 128.07, 126.97, 126.63, 126.59, 38.77, 33.58; ESI-HRMS (*m/z*) calcd $C_{18}H_{15}ClN_2O_2$ (M + H^+) 349.0714; found 349.0702.

2-Phenyl-*N*-(2-(pyridin-4-yl)ethyl)oxazole-4-carboxamide (18b). White solid, yield 50% from **16a**. ^{1}H NMR (600 MHz, $CDCl_3$) δ 8.56 (d, *J* = 5.9 Hz, 2H), 8.24 (s, 1H), 8.03-7.99 (m, 2H), 7.50-7.46 (m, 3H), 7.22 (d, *J* = 5.9 Hz, 2H), 7.13 (brs, 1H), 3.74 (q, *J* = 7.2 Hz, 2H), 2.97 (t, *J* = 7.2 Hz, 2H); ^{13}C NMR (151 MHz, $CDCl_3$) δ 160.88, 160.14, 149.38, 147.15, 140.17, 136.43, 130.51, 128.30, 125.99, 125.91, 123.53, 38.65, 34.65; ESI-HRMS (*m/z*) calcd $C_{17}H_{15}N_3O_2$ (M + H^+) 294.1237; found 294.1237.

***N*-(2-Chlorophenethyl)-5-phenyloxazole-2-carboxamide (18c).** White solid, yield 46% from **16b**. ^{1}H NMR (600 MHz, $CDCl_3$) δ 7.76-7.74 (m, 2H), 7.46-7.43 (m, 2H), 7.40-7.37 (m, 3H), 7.28-7.27 (m, 1H), 7.23-7.18 (m, 2H), 7.14 (brs, 1H), 3.75 (q, J = 6.8 Hz, 2H), 3.09 (t, J = 7.1 Hz, 2H); ^{13}C NMR (151 MHz, $CDCl_3$) δ 155.27, 154.21, 153.95, 136.09, 134.13, 130.95, 129.68, 129.48, 128.97, 128.21, 127.04, 126.88, 124.93, 122.54, 39.26, 33.34; ESI-HRMS (*m/z*) calcd $C_{18}H_{15}ClN_2O_2$ (M + H^+) 349.0714; found 349.0716.

5-Phenyl-*N*-(2-(pyridin-4-yl)ethyl)oxazole-2-carboxamide (18d). White solid, yield 53% from **16b**. ^{1}H NMR (600 MHz, $CDCl_3$) δ 8.56 (d, J = 4.6 Hz, 2H), 7.76-7.74 (m, 2H), 7.46-7.44 (m, 2H), 7.41-7.39 (m, 1H), 7.38 (s, 1H), 7.23 (d, J = 4.6 Hz, 2H), 7.12 (brs, 1H), 3.77 (q, J = 7.0 Hz, 2H), 2.98 (t, J = 7.0 Hz, 2H); ^{13}C NMR (151 MHz, $CDCl_3$) δ 154.67, 153.58, 153.37, 149.48, 146.75, 128.99, 128.41, 126.19, 124.37, 123.45, 121.95, 39.12, 34.39; ESI-HRMS (*m/z*) calcd $C_{17}H_{15}N_3O_2$ (M + H^+) 294.1237; found 294.1237.

***N*-(2-Chlorophenethyl)-5-phenyl-1,2,4-oxadiazole-3-carboxamide (18e).** White solid, yield 56% from **16c**. ^{1}H NMR (400 MHz, $CDCl_3$) δ 8.57 (d, J = 6.0 Hz, 2H), 8.17-8.15 (m, 2H), 7.67-7.63 (m, 1H), 7.58-7.54 (m, 2H), 7.21 (d, J = 6.0 Hz, 2H), 7.12 (brs, 1H), 3.81 (q, J = 7.0 Hz, 2H), 3.00 (t, J = 7.0 Hz, 2H); ^{13}C NMR (151 MHz, $CDCl_3$) δ 176.20, 163.28, 155.86, 135.36, 133.54, 132.84, 130.40, 129.13, 128.64, 127.73, 127.70, 126.51, 122.75, 38.78, 32.56; ESI-HRMS (*m/z*) calcd $C_{17}H_{14}ClN_3O_2$ (M + H^+) 350.0667; found 350.0655.

5-Phenyl-*N*-(2-(pyridin-4-yl)ethyl)-1,2,4-oxadiazole-3-carboxamide (18f). White solid, yield 63% from **16c**. ^{1}H NMR (600 MHz, DMSO-d_6) δ 9.15 (t, J = 7.2 Hz, 1H), 8.44 (d, J = 5.9 Hz, 2H), 8.12 (d, J = 7.0 Hz, 2H), 7.72 (t, J = 7.0 Hz, 1H), 7.64 (t, J = 7.0 Hz, 2H), 7.25 (d, J = 5.9 Hz, 2H), 3.55 (q, J = 7.2 Hz, 2H), 2.88 (t, J = 7.2 Hz, 2H); ^{13}C NMR (151 MHz, DMSO-d_6) δ 176.41, 164.62, 156.57, 149.99, 148.45, 134.20, 130.13, 128.52, 124.71, 123.42, 40.49, 34.21; ESI-HRMS (*m/z*) calcd $C_{16}H_{14}N_4O_2$ (M + H^+) 317.1009; found 317.1006.

***N*-(2-Chlorophenethyl)-3-phenyl-1,2,4-oxadiazole-5-carboxamide (18g).** White solid, yield 62% from **16d**. ^{1}H NMR (600 MHz, $CDCl_3$) δ 8.09-8.08 (m, 2H),

7.56-7.54 (m, 1H), 7.52-7.49 (m, 2H), 7.41-7.39 (m, 1H), 7.29-7.26 (m, 1H), 7.25-7.22 (m, 3H), 3.80 (q, *J* = 7.1 Hz, 2H), 3.13 (t, *J* = 7.1 Hz, 2H); ^{13}C NMR (151 MHz, $CDCl_3$) δ 168.68, 168.56, 153.11, 135.66, 134.13, 131.74, 130.95, 129.80, 128.97, 128.44, 127.53, 127.18, 125.78, 39.71, 33.07; ESI-HRMS (*m/z*) calcd $C_{17}H_{14}ClN_3O_2$ (M + H^+) 350.0667; found 350.0664.

3-Phenyl-*N*-(2-(pyridin-4-yl)ethyl)-1,2,4-oxadiazole-5-carboxamide (18h). White solid, yield 52% from **16d**. ^{1}H NMR (600 MHz, $CDCl_3$) δ 8.55 (dd, *J* = 4.5, 1.4 Hz, 2H), 8.06-8.05 (m, 2H), 7.55-7.52 (m, 1H), 7.50-7.48 (m, 2H), 7.44 (brs, 1H), 7.19 (dd, *J* = 4.5, 1.4 Hz, 2H), 3.80 (q, *J* = 7.0 Hz, 2H), 3.00 (t, *J* = 7.0 Hz, 2H); ^{13}C NMR (151 MHz, $CDCl_3$) δ 168.71, 168.44, 153.24, 150.04, 147.07, 131.80, 128.97, 127.48, 125.64, 124.04, 40.18, 34.67; ESI-HRMS (*m/z*) calcd $C_{16}H_{14}N_4O_2$ (M + H^+) 317.1009; found 317.1006.

***N*-(2-Chlorophenethyl)-5-phenyl-1,3,4-oxadiazole-2-carboxamide (18i).** White solid, yield 51% from **16e**. ^{1}H NMR (600 MHz, $CDCl_3$) δ 8.15 (d, *J* = 8.3 Hz, 2H), 7.59 (t, *J* = 8.3 Hz, 1H), 7.53 (t, *J* = 8.3 Hz, 2H), 7.38-7.37 (m, 1H), 7.34 (brs, 1H), 7.27-7.26 (m, 1H), 7.23-7.19 (m, 2H), 3.80 (q, *J* = 7.0 Hz, 2H), 3.12 (t, *J* = 7.0 Hz, 2H); ^{13}C NMR (151 MHz, DMSO-d_6) δ 165.41, 158.90, 153.48, 136.83, 133.65, 133.12, 131.59, 130.01, 129.76, 128.83, 127.80, 127.51, 123.26, 39.33, 32.88; ESI-HRMS (*m/z*) calcd $C_{17}H_{14}ClN_3O_2$ (M + H^+) = 328.0847; found 328.0846.

5-Phenyl-*N*-(2-(pyridin-4-yl)ethyl)-1,3,4-oxadiazole-2-carboxamide (18j). White solid, yield 49% from **16e**. ^{1}H NMR (600 MHz, $CDCl_3$) δ 8.56 (dd, *J* = 4.5, 1.4 Hz, 2H), 8.16-8.14 (m, 2H), 7.61-7.59 (m, 1H), 7.56-7.53 (m, 2H), 7.28 (brt, 1H), 7.21 (dd, *J* = 4.5, 1.4 Hz, 2H), 3.81 (q, *J* = 7.0 Hz, 2H), 2.99 (t, *J* = 7.0 Hz, 2H); ^{13}C NMR (151 MHz, $CDCl_3$) δ 166.60, 158.28, 153.41, 150.10, 147.03, 132.69, 129.20, 127.49, 124.00, 122.79, 40.01, 34.84; ESI-HRMS (*m/z*) calcd $C_{16}H_{14}N_4O_2$ (M + H^+) 317.1009; found 317.1014.

***N*-(2-Chlorophenethyl)biphenyl-4-carboxamide (20a).** White solid, yield 74%. ^{1}H NMR (600 MHz, $CDCl_3$) δ 7.79 (d, *J* = 8.4 Hz, 2H), 7.64 (d, *J* = 8.4 Hz, 2H), 7.61-7.59 (m, 2H), 7.47-7.44 (m, 2H), 7.40-7.37 (m, 2H), 7.29 (dd, *J* = 7.3, 1.9 Hz, 1H), 7.24-7.18 (m, 2H), 6.29 (brs, 1H), 3.77 (q, *J* = 6.8 Hz, 2H), 3.12 (t, *J* = 6.8 Hz,

2H); ^{13}C NMR (151 MHz, $CDCl_3$) δ 166.64, 143.62, 139.39, 136.05, 133.52, 132.60, 130.51, 129.08, 128.28, 127.53, 127.35, 126.75, 126.60, 126.56, 126.47, 39.20, 32.72; ESI-HRMS (*m/z*) calcd $C_{21}H_{18}ClNO$ (M + H^+) 336.1150; found 336.1151.

***N*-(2-(Pyridin-4-yl)ethyl)biphenyl-4-carboxamide (20b).** White solid, yield 74%. ^{1}H NMR (600 MHz, $CDCl_3$) δ 8.53 (d, *J* = 4.6 Hz, 2H), 7.78 (d, *J* = 8.3 Hz, 2H), 7.64 (d, *J* = 8.3 Hz, 2H), 7.60 (d, *J* = 7.2 Hz, 2H), 7.47-7.44 (m, 2H), 7.39-7.37 (m, 1H), 7.17 (d, *J* = 4.6 Hz, 2H), 6.34 (brs, 1H), 3.76 (q, *J* = 7.0 Hz, 2H), 2.97 (t, *J* = 7.0 Hz, 2H); ^{13}C NMR (151 MHz, $CDCl_3$) δ 166.71, 149.39, 147.43, 143.86, 139.29, 132.31, 128.31, 127.43, 126.73, 126.67, 126.56, 123.59, 39.69, 34.53; ESI-HRMS (*m/z*) calcd $C_{20}H_{18}N_2O$ (M + H^+) 303.1492; found 303.1487.

Synthesis of 5-phenylpicolinic acid (23a) and 6-phenylnicotinic acid (23b). A mixture of 5-bromo-pyridine-2-carboxylic acid (**22a**) or 6-bromonicotinic acid (**22b**) (1.98 g, 9.9 mmol), phenylboronic acid **21** (1.6 g, 13.2 mmol), K_2CO_3 (2.46 g, 17.82 mmol) and $Pd(PPh_3)_2Cl_2$ (0.69 g, 1.2 mmol) in dioxane-water (v:v = 3:1, 40 mL) was stirred at 110 °C under N_2 atmosphere for 12 h. The reaction mixture was cooled to room temperature, adjusted to pH = 9-10 with saturated aqueous solution of $NaHCO_3$, and filtered. The filtrate was washed with Et_2O. The aqueous layer was adjusted to pH = 4-5 with 1N HCl and extracted with ethyl acetate. The combined organic layer was dried over Na_2SO_4 and concentrated to give the crude product **23a** as white solid (61% yield) or **23b** as white solid (69% yield), which was used for the next step without purification.

***N*-(2-Chlorophenethyl)-5-phenylpicolinamide (24a).** White solid, yield 77%. ^{1}H NMR (600 MHz, $CDCl_3$) δ 8.75 (d, *J* = 1.9 Hz, 1H), 8.28 (d, *J* = 8.1 Hz, 1H), 8.22 (brs, 1H), 8.05 (dd, *J* = 8.1, 1.9 Hz, 1H), 7.62 (d, *J* = 7.3 Hz, 2H), 7.51 (t, *J* = 7.3 Hz, 2H), 7.45 (t, *J* = 7.3 Hz, 1H), 7.38 (dd, *J* = 7.5, 1.6 Hz, 1H), 7.30 (dd, *J* = 7.2, 1.8 Hz, 1H), 7.22-7.17 (m, 2H), 3.78 (q, *J* = 7.1 Hz, 2H), 3.12 (t, *J* = 7.1 Hz, 2H); ^{13}C NMR (151 MHz, $CDCl_3$) δ 160.38, 144.61, 142.64, 135.09, 133.06, 132.65, 131.53, 130.25, 127.01, 125.67, 125.24, 124.70, 124.05, 123.28, 122.99, 118.23, 35.18, 29.72; ESI-HRMS (*m/z*) calcd $C_{20}H_{17}ClN_2O$ (M + H^+) 341.1260; found 341.1263.

5-Phenyl-*N*-(2-(pyridin-4-yl)ethyl)picolinamide (24b). White solid, yield 73%.

^{1}H NMR (600 MHz, $CDCl_3$) δ 8.73 (d, J = 2.0 Hz, 1H), 8.54 (d, J = 5.8 Hz, 2H), 8.24 (d, J = 8.1 Hz, 1H), 8.13 (brs, 1H), 8.02 (dd, J = 8.1, 2.0 Hz, 1H), 7.60 (d, J = 7.3 Hz, 2H), 7.50 (t, J = 7.3 Hz, 2H), 7.44 (t, J = 7.3 Hz, 2H), 7.19 (d, J = 5.8 Hz, 2H), 3.78 (q, J = 7.1 Hz, 2H), 2.97 (t, J = 7.1 Hz, 2H); ^{13}C NMR (151 MHz, $CDCl_3$) δ 163.74, 149.36, 147.66, 147.33, 146.04, 138.61, 136.31, 134.95, 128.62, 128.11, 126.63, 123.54, 121.61, 39.03, 34.67; ESI-HRMS (*m/z*) calcd $C_{19}H_{17}N_3O$ (M + H^+) 304.1444; found 304.1448.

***N*-(2-Chlorophenethyl)-6-phenylnicotinamide (24c).** White solid, yield 72%. ^{1}H NMR (600 MHz, $CDCl_3$) δ 8.95 (s, 1H), 8.14 (d, J = 8.3 Hz, 1H), 8.02 (d, J = 7.6 Hz, 2H), 7.81 (d, J = 8.3 Hz, 1H), 7.50 (t, J = 7.6 Hz, 2H), 7.47-7.46 (m, 1H), 7.40 (d, J = 7.7 Hz, 1H), 7.29 (d, J = 7.3 Hz, 1H), 7.25-7.19 (m, 2H), 6.24 (brs, 1H), 3.80 (q, J = 6.8 Hz, 2H), 3.13 (t, J = 6.8 Hz, 2H); ^{13}C NMR (151 MHz, $CDCl_3$) δ 165.10, 159.31, 147.04, 137.65, 135.79, 135.42, 135.02, 133.50, 132.99, 130.50, 129.17, 128.29, 127.70, 127.36, 126.58, 119.60, 39.32, 32.57; ESI-HRMS (*m/z*) calcd $C_{20}H_{17}ClN_2O$ (M + H^+) 337.1102; found 337.1102.

6-Phenyl-*N*-(2-(pyridin-4-yl)ethyl)nicotinamide (24d). White solid, yield 73%. ^{1}H NMR (600 MHz, $CDCl_3$) δ 8.97 (d, J = 2.0 Hz, 1H), 8.56 (d, J = 5.9 Hz, 2H), 8.15 (dd, J = 8.3, 2.0 Hz, 1H), 8.05-8.04 (m, 2H), 7.83 (d, J = 8.3 Hz, 1H), 7.53-7.48 (m, 3H), 7.21 (d, J = 5.9 Hz, 2H), 6.33 (brs, 1H), 3.81 (q, J = 7.0 Hz, 2H), 3.01 (t, J = 7.0 Hz, 2H); ^{13}C NMR (151 MHz, $CDCl_3$) δ 165.74, 160.00, 149.95, 147.87, 147.71, 138.20, 135.91, 129.79, 128.86, 128.09, 127.15, 124.14, 120.07, 40.34, 35.06; ESI-HRMS (*m/z*) calcd $C_{19}H_{17}N_3O$ (M + H^+) 304.1444; found 304.1445.

Synthesis of 6-phenylpyrimidine-4-carboxylic acid (26a) and 4-phenylpyrimidine-2-carboxylic acid (26b).[36] The mixture of **25a** or **25b** (5 g, 0.025 mol) and 20% aqueous solution of H_2SO_4 (100 mL) was refluxed at 100 °C for 5-10 h. After TLC showed the completion of the reaction, the reaction mixture was poured into stirring ice water. The precipitate was filtered and dried to obtain crude product **26a** as white solid (34% yield) or **26b** as white solid (39% yield), which were used for the next step without purification.

***N*-(2-Chlorophenethyl)-6-phenylpyrimidine-4-carboxamide (27a).** White

solid, yield 71%. ^{1}H NMR (600 MHz, $CDCl_3$) δ 9.20 (d, J = 1.0 Hz, 1H), 8.54 (d, J = 1.0 Hz, 1H), 8.20-8.18 (m, 2H), 8.15 (brs, 1H), 7.54-7.52 (m, 3H), 7.38 (dd, J = 7.2, 1.6 Hz, 1H), 7.28-7.27 (m, 1H), 7.23-7.18 (m, 2H), 3.79 (q, J = 7.0 Hz, 2H), 3.12 (t, J = 7.0 Hz, 2H); ^{13}C NMR (151 MHz, $CDCl_3$) δ 165.77, 162.48, 157.27, 155.99, 149.43, 146.95, 135.36, 131.04, 128.52, 126.80, 123.46, 113.33, 39.12, 34.45; ESI-HRMS (*m/z*) calcd $C_{18}H_{16}N_4O$ (M + H^+) 305.1397; found 305.1401.

4-Phenyl-*N*-(2-(pyridin-4-yl)ethyl)pyrimidine-2-carboxamide (27b). White solid, yield 73%. ^{1}H NMR (600 MHz, $CDCl_3$) δ 9.20 (s, 1H), 8.54 (d, J = 4.6 Hz, 2H), 8.52 (s, 1H), 8.19-8.18 (m, 2H), 8.13 (brs, 1H), 7.54-7.53 (m, 3H), 7.18 (d, J = 4.6 Hz, 2H), 3.79 (q, J = 7.2 Hz, 2H), 2.97 (t, J = 7.2 Hz, 2H); ^{13}C NMR (151 MHz, $CDCl_3$) δ 165.67, 162.45, 157.25, 156.27, 135.64, 135.46, 133.59, 130.98, 130.33, 129.11, 128.51, 127.58, 126.80, 126.42, 113.35, 38.66, 32.83; ESI-HRMS (*m/z*) calcd $C_{19}H_{16}ClN_3O$ (M + H^+) 360.0874; found 360.0874.

***N*-Phenethyl-5-phenylpicolinamide (28a).** White solid, yield 71%. ^{1}H NMR (600 MHz, DMSO-d_6) δ 8.91 (d, J = 2.0 Hz, 1H), 8.81 (brs, 1H), 8.25 (dd, J = 8.1, 2.0 Hz, 1H), 8.08 (d, J = 8.1 Hz, 1H), 7.78 (d, J = 7.6 Hz, 2H), 7.52 (t, J = 7.6 Hz, 2H), 7.45 (t, J = 7.6 Hz, 1H), 7.29-7.27 (m, 2H), 7.24-7.23 (m, 2H), 7.20-7.17 (m, 1H), 3.56 (q, J = 7.1 Hz, 2H), 2.87 (t, J = 7.1 Hz, 2H); ^{13}C NMR (151 MHz, DMSO-d_6) δ 163.95, 149.27, 146.88, 139.83, 138.31, 136.66, 135.97, 129.66, 129.16, 129.04, 128.80, 127.59, 126.55, 122.38, 40.80, 35.59; ESI-HRMS (*m/z*) calcd $C_{20}H_{18}N_2O$ (M + H^+) 303.1492; found 303.1496.

***N*-(3-Chlorophenethyl)-5-phenylpicolinamide (28b).** White solid, yield 74%. ^{1}H NMR (600 MHz, $CDCl_3$) δ 8.74 (d, J = 2.2 Hz, 1H), 8.25 (d, J = 8.1 Hz, 1H), 8.15 (brt, 1H), 8.02 (dd, J = 8.1, 2.2 Hz, 1H), 7.61-7.60 (m, 2H), 7.50 (t, J = 7.5 Hz, 2H), 7.45-7.43 (m, 1H), 7.26-7.21 (m, 3H), 7.15 (d, J = 7.2 Hz, 1H), 3.74 (q, J = 7.2 Hz, 2H), 2.94 (t, J = 7.2 Hz, 2H); ^{13}C NMR (151 MHz, $CDCl_3$) δ 164.28, 148.44, 146.60, 140.98, 139.10, 136.96, 135.51, 134.35, 129.84, 129.19, 128.94, 128.67, 127.22, 126.96, 126.70, 122.20, 40.49, 35.65; ESI-HRMS (*m/z*) calcd $C_{20}H_{17}ClN_2O$ (M + H^+) 337.1102; found 337.1108.

***N*-(4-Chlorophenethyl)-5-phenylpicolinamide (28c).** White solid, yield 75%. ^{1}H NMR (600 MHz, $CDCl_3$) δ 8.73 (d, J = 1.8 Hz, 1H), 8.25 (d, J = 8.1 Hz, 1H), 8.13 (brs, 1H), 8.01 (dd, J = 8.1 Hz, 1.8 Hz, 1H), 7.60 (d, J = 7.6 Hz, 2H), 7.50 (t, J = 7.6 Hz, 2H), 7.44 (t, J = 7.6 Hz, 1H), 7.28 (d, J = 8.3 Hz, 2H), 7.19 (d, J = 8.3 Hz, 2H), 3.73 (q, J = 7.2 Hz, 2H), 2.93 (t, J = 7.2 Hz, 2H); ^{13}C NMR (151 MHz, $CDCl_3$) δ 164.22, 148.48, 146.59, 139.06, 137.42, 136.95, 135.49, 132.28, 130.12, 129.20, 128.71, 128.67, 127.22, 122.19, 40.57, 35.32; ESI-HRMS (*m/z*) calcd $C_{20}H_{17}ClN_2O$ (M + H^+) 337.1102; found 337.1102.

***N*-(2-Fluorophenethyl)-5-phenylpicolinamide (28d).** White solid, yield 71%. ^{1}H NMR (600 MHz, $CDCl_3$) δ 8.73 (d, J = 1.5 Hz, 1H), 8.24 (d, J = 8.0 Hz, 1H), 8.16 (brs, 1H), 8.00 (dd, J = 8.0, 1.5 Hz, 1H), 7.59 (d, J = 7.6 Hz, 2H), 7.49 (t, J = 7.6 Hz, 2H), 7.43 (t, J = 7.6 Hz, 1H), 7.25-7.22 (m, 1H), 7.21-7.19 (m, 1H), 7.08-7.06 (m, 1H), 7.05-7.02 (m, 1H), 3.75 (q, J = 7.1 Hz, 2H), 3.00 (t, J = 7.1 Hz, 2H); ^{13}C NMR (151 MHz, DMSO-d_6) δ 164.08, 161.23, 149.25, 146.93, 138.34, 136.69, 136.02, 131.63, 129.72, 129.22, 128.77, 127.65, 126.49, 124.84, 122.45, 115.60, 40.49, 28.98; ESI-HRMS (*m/z*) calcd $C_{20}H_{17}FN_2O$ (M + H^+) 321.1398; found 321.1399.

***N*-(3-Fluorophenethyl)-5-phenylpicolinamide (28e).** White solid, yield 74%. ^{1}H NMR (600 MHz, $CDCl_3$) δ 8.76 (d, J = 1.8 Hz, 1H), 8.28 (d, J = 8.1, 1H), 8.17 (brt, 1H), 8.05 (dd, J = 8.1, 1.8 Hz, 1H), 7.63 (d, J = 7.3 Hz, 2H), 7.53 (t, J = 7.3 Hz, 2H), 7.48-7.47 (m, 1H), 7.32-7.29 (m, 1H), 7.07 (d, J = 7.6 Hz, 1H), 7.01-6.99 (m, 1H), 6.97-6.95 (m, 1H), 3.78 (q, J = 7.2 Hz, 2H), 2.99 (t, J = 7.2 Hz, 2H); ^{13}C NMR (151 MHz, $CDCl_3$) δ 163.67, 162.10, 147.81, 146.02, 140.89, 138.50, 136.35, 134.95, 129.45, 128.62, 128.09, 126.64, 123.85, 121.62, 115.07, 112.81, 39.89, 35.10; ESI-HRMS (*m/z*) calcd $C_{20}H_{17}FN_2O$ (M + H^+) 321.1398; found 321.1399.

***N*-(4-Fluorophenethyl)-5-phenylpicolinamide (28f).** White solid, yield 78%. ^{1}H NMR (600 MHz, $CDCl_3$) δ 8.74 (d, J = 2.3 Hz, 1H), 8.25 (d, J = 8.1 Hz, 1H), 8.11 (brs, 1H), 8.02 (dd, J = 8.1, 2.3 Hz, 1H), 7.62-7.60 (m, 2H), 7.52-7.49 (m, 2H), 7.46-7.43 (m, 1H), 7.23-7.21 (m, 2H), 7.02-6.99 (m, 2H), 3.73 (q, J = 7.2 Hz, 2H), 2.94 (t, J = 7.2 Hz, 2H); ^{13}C NMR (151 MHz, $CDCl_3$) δ 163.62, 160.77, 147.91, 146.01, 138.46, 136.38, 134.90, 134.00, 129.58, 128.60, 128.07, 126.63, 121.58, 114.78,

40.18, 34.56; ESI-HRMS (*m/z*) calcd $C_{20}H_{17}FN_2O$ (M + H^+) 321.1398; found 321.14.

5-Phenyl-*N*-(2-(pyridin-2-yl)ethyl)picolinamide (28g). White solid, yield 74%. ^{1}H NMR (600 MHz, $CDCl_3$) δ 8.74 (d, *J* = 2.0 Hz, 1H), 8.59 (d, *J* = 4.7 Hz, 1H), 8.51 (brt, 1H), 8.24 (d, *J* = 8.1 Hz, 1H), 7.99 (dd, *J* = 8.1, 2.0 Hz, 1H), 7.62-7.58 (m, 3H), 7.48 (t, *J* = 7.6 Hz, 2H), 7.42 (t, *J* = 7.6 Hz, 1H), 7.21 (d, *J* = 7.6 Hz, 1H), 7.16-7.13 (m, 1H), 3.91 (q, *J* = 6.5 Hz, 2H), 3.14 (t, *J* = 6.5 Hz, 2H); ^{13}C NMR (151 MHz, $CDCl_3$) δ 164.28, 159.28, 149.34, 148.76, 146.66, 138.86, 137.07, 136.53, 135.36, 129.16, 128.58, 127.20, 123.37, 122.14, 121.52, 38.84, 37.57; ESI-HRMS (*m/z*) calcd $C_{19}H_{17}N_3O$ (M + H^+) 304.1444; found 304.1448.

5-Phenyl-*N*-(2-(pyridin-3-yl)ethyl)picolinamide (28h). White solid, yield 67%. ^{1}H NMR (600 MHz, $CDCl_3$) δ 8.73 (dd, *J* = 2.3, 0.8 Hz, 1H), 8.53 (d, *J* = 1.8 Hz, 1H), 8.50 (dd, *J* = 4.8, 1.8 Hz, 1H), 8.24 (dd, *J* = 8.1, 0.8 Hz, 1H), 8.15 (brs, 1H), 8.02 (dd, *J* = 8.1, 2.3 Hz, 1H), 7.61-7.60 (m, 3H), 7.51-7.49 (m, 2H), 7.46-7.43 (m, 1H), 7.25-7.24 (m, 1H), 3.77 (q, *J* = 7.0 Hz, 2H), 2.98 (t, *J* = 7.0 Hz, 2H); ^{13}C NMR (151 MHz, $CDCl_3$) δ 164.32, 150.19, 148.37, 148.04, 146.62, 139.14, 136.94, 136.17, 135.49, 134.35, 129.18, 128.66, 127.21, 123.45, 122.16, 40.35, 33.15; ESI-HRMS (*m/z*) calcd $C_{19}H_{17}N_3O$ (M + H^+) 304.1444; found 304.1449.

***N*-(4-Hydroxyphenethyl)-5-phenylpicolinamide (28i).** White solid, yield 74%. ^{1}H NMR (600 MHz, $CDCl_3$) δ 8.75 (d, *J* = 1.7 Hz, 1H), 8.28 (d, *J* = 8.1 Hz, 1H), 8.21 (brs, 1H), 8.05 (dd, *J* = 8.1, 1.7 Hz, 1H), 7.62-7.60 (m, 2H), 7.51 (t, *J* = 7.5 Hz, 2H), 7.45 (t, *J* = 7.5 Hz, 1H), 7.13 (d, *J* = 8.4 Hz, 2H), 6.80 (d, *J* = 8.4 Hz, 2H), 3.72 (q, *J* = 7.0 Hz, 2H), 2.90 (t, *J* = 7.0 Hz, 2H); ^{1}C NMR (151 MHz, DMSO-d_6) δ 163.28, 155.47, 148.67, 146.29, 137.68, 136.06, 135.39, 131.35, 129.31, 129.08, 128.57, 127.00, 121.78, 114.99, 40.53, 34.19; ESI-HRMS (*m/z*) calcd $C_{20}H_{18}N_2O_2$ (M + H^+) 337.1102; found 337.1102.

***N*-(4-Aminophenethyl)-5-phenylpicolinamide (28j).** White solid, yield 72%. ^{1}H NMR (600 MHz, $CDCl_3$) δ 8.74 (d, *J* = 2.1 Hz, 1H), 8.26 (d, *J* = 8.0 Hz, 1H), 8.12 (brs, 1H), 8.01 (dd, *J* = 8.0, 2.1 Hz, 1H), 7.60 (d, *J* = 7.7 Hz, 2H), 7.50 (t, *J* = 7.7 Hz, 2H), 7.44 (t, *J* = 7.7 Hz, 1H), 7.06 (d, *J* = 8.2 Hz, 2H), 6.66 (d, *J* = 8.2 Hz, 2H), 3.70 (q, *J* = 7.2 Hz, 2H), 3.63 (brs, 2H), 2.85 (t, *J* = 7.2 Hz, 2H); ^{13}C NMR (151 MHz,

$CDCl_3$) δ 164.14, 148.74, 146.57, 144.78, 138.90, 137.06, 135.42, 129.58, 129.17, 128.89, 128.59, 127.21, 122.14, 115.42, 41.03, 35.08; ESI-HRMS (*m/z*) calcd $C_{20}H_{19}N_3O$ (M + H^+) 318.1601; found 318.1603.

***N*-(4-Methylphenethyl)-5-phenylpicolinamide (28k).** White solid, yield 70%. ^{1}H NMR (600 MHz, $CDCl_3$) δ 8.75 (d, *J* = 2.1 Hz, 1H), 8.27 (d, *J* = 8.1 Hz, 1H), 8.16 (brs, 1H), 8.02 (dd, *J* = 8.1, 2.1 Hz, 1H), 7.61 (d, *J* = 7.3 Hz, 2H), 7.51 (t, *J* = 7.3 Hz, 2H), 7.45 (t, *J* = 7.3 Hz, 1H), 7.18-7.14 (m, 4H), 3.75 (q, *J* = 7.2 Hz, 2H), 2.94 (t, *J* = 7.2 Hz, 2H), 2.34 (s, 3H); ^{13}C NMR (151 MHz, $CDCl_3$) δ 164.21, 148.63, 146.58, 138.97, 137.01, 135.94, 135.84, 135.62, 135.47, 129.29, 129.19, 128.65, 127.22, 122.19, 40.89, 35.52, 21.02; ESI-HRMS (*m/z*) calcd $C_{21}H_{20}N_2O$ (M + H^+) 317.1648; found 317.1648.

***N*-(4-Nitrophenethyl)-5-phenylpicolinamide (28l).** White solid, yield 63%. ^{1}H NMR (600 MHz, $CDCl_3$) δ 8.72 (d, *J* = 1.6 Hz, 1H), 8.23 (d, *J* = 8.0 Hz, 1H), 8.17-8.15 (m, 3H), 8.02 (dd, *J* = 8.0, 1.6 Hz, 1H), 7.59 (d, *J* = 7.3 Hz, 2H), 7.49 (t, *J* = 7.3 Hz, 2H), 7.46-7.41 (m, 3H), 3.79 (q, *J* = 7.1 Hz, 2H), 3.08 (t, *J* = 7.1 Hz, 2H); ^{13}C NMR (151 MHz, $CDCl_3$) δ 164.39, 148.22, 146.85, 146.75, 146.64, 139.24, 136.84, 135.53, 129.63, 129.21, 128.73, 127.20, 123.80, 122.21, 40.14, 35.85; ESI-HRMS (*m/z*) calcd $C_{20}H_{17}N_3O_3$ (M + H^+) 348.1343; found 348.1339.

5-Bromo-*N*-(2-fluorophenethyl)picolinamide (29). White solid (246 mg, 76%) ^{1}H NMR (600 MHz, $CDCl_3$) δ 8.57 (d, *J* = 2.2 Hz, 1H), 8.10 (d, *J* = 8.3 Hz, 1H), 8.00 (brs, 1H), 7.96 (dd, *J* = 8.3, 2.2 Hz, 1H), 7.24-7.20 (m, 2H), 7.09-7.02 (m, 2H), 3.72 (q, *J* = 7.1 Hz, 2H), 2.99 (t, *J* = 7.1 Hz, 2H); ESI-HRMS (*m/z*) calcd $C_{14}H_{12}BrFN_2O$ (M + H^+) 323.1090; found 323.1093.

General procedure for the synthesis of 30a-r exemplified by *N*-(2-fluorophenethyl)-5-(furan-2-yl)picolinamide (30a). A mixture of compound **49** (161 mg, 0.5 mmol), furan-2-yl boronic acid (75 mg, 0.66 mmol), K_2CO_3 (124 mg, 0.9 mmol) and $Pd(PPh_3)_2Cl_2$ (35 mg, 0.05 mmol) in dioxane-water (v:v=3:1, 20 mL) was stirred at 110 °C under N_2 atmosphere for 12 h. The reaction mixture was cooled to room temperature, and extracted with ethyl acetate. The combined organic layer was dried over anhydrous Na_2SO_4. After removal of the solvent in vacuo, the residue

was purified by flash chromatography to yield compound **30a** as a white solid (68% yield). ^{1}H NMR (600 MHz, $CDCl_3$) δ 8.84 (d, J = 2.2 Hz, 1H), 8.08 (dd, J = 8.3, 2.2 Hz, 1H), 7.73 (d, J = 8.3 Hz, 1H), 7.57 (d, J = 1.7 Hz, 1H), 7.25-7.22 (m, 2H), 7.14 (d, J = 3.4 Hz, 1H), 7.11-7.10 (m, 1H), 7.09-7.06 (m, 1H), 6.56 (dd, J = 3.4, 1.7 Hz, 1H), 6.26 (brs, 1H), 3.74 (q, J = 6.6 Hz, 2H), 3.01 (t, J = 6.6 Hz, 2H); ^{13}C NMR (151 MHz, $CDCl_3$) δ 164.79, 160.50, 152.20, 150.78, 147.11, 143.65, 135.26, 130.60, 128.00, 127.26, 125.00, 123.82, 117.50, 114.89, 111.81, 109.89, 39.61, 28.50; ESI-HRMS (*m/z*) calcd $C_{18}H_{15}FN_2O_2$ (M + H^+) 311.1190; found 311.1190.

***N*-(2-Fluorophenethyl)-5-(furan-3-yl)picolinamide (30b).** White solid, yield 65%. ^{1}H NMR (600 MHz, DMSO-d_6) δ 8.91 (d, J = 2.1 Hz, 1H), 8.85 (t, J = 6.8 Hz, 1H), 8.45 (s, 1H), 8.20 (dd, J = 8.1, 2.1 Hz, 1H), 8.02 (d, J = 8.1 Hz, 1H), 7.85 (t, J = 1.7 Hz, 1H), 7.32 (td, J = 7.6, 1.7 Hz, 1H), 7.28-7.25 (m, 1H), 7.15-7.13 (m, 3H), 3.56 (q, J = 6.8 Hz, 2H), 2.92 (t, J = 6.8 Hz, 2H); ^{13}C NMR (151 MHz, DMSO-d_6) δ 163.45, 160.44, 148.03, 145.23, 144.76, 140.94, 133.72, 130.97, 130.24, 128.12, 125.83, 124.19, 122.08, 121.80, 114.96, 108.35, 39.87, 28.34; ESI-HRMS (*m/z*) calcd $C_{18}H_{15}FN_2O_2$ (M + H+) 311.1190; found 311.1191.

***N*-(2-Fluorophenethyl)-5-(thiophen-2-yl)picolinamide (30c).** White solid, yield 67%. ^{1}H NMR (600 MHz, $CDCl_3$) δ 8.77 (d, J = 2.3 Hz, 1H), 8.19 (d, J = 8.1 Hz, 1H), 8.09 (brs, 1H), 8.00 (dd, J = 8.1, 2.3 Hz, 1H), 7.44 (dd, J = 3.6, 1.0 Hz, 1H), 7.42 (dd, J = 5.1, 1.0 Hz, 1H), 7.25-7.21 (m, 2H), 7.15 (dd, J = 5.1, 3.6 Hz, 1H), 7.08 (t, J = 7.4, 1H), 7.07-7.02 (m, 1H), 3.75 (q, J = 7.0 Hz, 2H), 3.01 (t, J = 7.0 Hz, 2H); ^{13}C NMR (151 MHz, $CDCl_3$) δ 164.07, 161.32, 148.40, 145.12, 139.59, 133.79, 132.68, 131.06, 128.46, 128.26, 126.92, 125.84, 125.05, 124.14, 122.29, 115.34, 39.53, 29.34; ESI-HRMS (*m/z*) calcd $C_{18}H_{15}FN_2OS$ (M + H^+) 327.0962; found 327.0962.

***N*-(2-Fluorophenethyl)-5-(thiophen-3-yl)picolinamide (30d).** White solid, yield 61%. ^{1}H NMR (600 MHz, DMSO-d_6) δ 8.98 (d, J = 1.6 Hz, 1H), 8.84 (t, J = 6.0 Hz, 1H), 8.28 (dd, J = 8.1, 2.2 Hz, 1H), 8.17-8.16 (m, 1H), 8.01 (d, J = 8.1 Hz, 1H), 7.72 (dd, J = 5.0, 2.9 Hz, 1H), 7.70 (dd, J = 5.0, 1.6 Hz, 1H), 7.32-7.28 (m, 1H), 7.26-7.21 (m, 1H), 7.15-7.08 (m, 2H), 3.54 (q, J = 7.1 Hz, 2H), 2.90 (t, J = 7.1 Hz, 2H); ^{13}C NMR (151 MHz, $CDCl_3$) δ 163.64, 160.41, 147.59, 145.31, 137.42, 133.91,

133.19, 131.48, 130.51, 127.90, 127.69, 126.73, 125.21, 123.58, 121.77, 114.76, 38.92, 28.76; ESI-HRMS (*m/z*) calcd $C_{18}H_{15}FN_2OS$ (M + H^+) 327.0962; found 327.0963.

***N*-(2-Fluorophenethyl)-3,4'-bipyridine-6-carboxamide (30e).** White solid, yield 67%. ^{1}H NMR (600 MHz, $CDCl_3$) δ 8.78 (d, *J* = 1.8 Hz, 1H), 8.74 (d, *J* = 5.9 Hz, 2H), 8.30 (d, *J* = 8.1 Hz, 1H), 8.16 (brs, 1H), 8.07 (dd, *J* = 8.1, 2.2 Hz, 1H), 7.52 (dd, *J* = 4.6, 1.8 Hz, 2H), 7.26-7.23 (m, 1H), 7.23-7.19 (m, 1H), 7.08 (t, *J* = 7.2 Hz, 1H), 7.06-7.02 (m, 1H), 3.76 (q, *J* = 7.0 Hz, 2H), 3.01 (t, *J* = 7.0 Hz, 2H). ^{13}C NMR (151 MHz, $CDCl_3$) δ 163.78, 162.12, 150.67, 150.12, 146.47, 144.36, 136.11, 135.64, 132.10, 131.04, 128.30, 124.18, 122.39, 121.55, 115.30, 39.60, 29.32; ESI-HRMS (*m/z*) calcd $C_{19}H_{16}FN_3O$ (M + H^+) 322.1350; found 322.1354.

***N*-(2-Fluorophenethyl)-5-(1*H*-pyrazol-4-yl)picolinamide (30f).** White solid, yield 66%. ^{1}H NMR (600 MHz, $CDCl_3$) δ 8.69 (d, *J* = 1.8 Hz, 1H), 8.20 (d, *J* = 8.1 Hz, 1H), 8.12 (brs, 1H), 7.96 (s, 2H), 7.92 (dd, *J* = 8.1, 1.8 Hz, 1H), 7.25-7.21 (m, 2H), 7.09-7.03 (m, 2H), 3.75 (q, *J* = 7.1 Hz, 2H), 3.01 (t, *J* = 7.1 Hz, 2H); ^{13}C NMR (151 MHz, DMSO-d_6) δ 163.58, 160.38, 147.02, 144.76, 136.63, 132.92, 131.26, 130.99, 128.09, 126.61, 125.87, 124.19, 121.81, 117.07, 114.96, 38.83, 28.36; ESI-HRMS (*m/z*) calcd $C_{17}H_{15}FN_4O$ (M + H^+) 311.1303; found 311.1300.

***N*-(2-Fluorophenethyl)-5-(2-fluorophenyl)picolinamide (30g).** White solid, yield 69%. ^{1}H NMR (600 MHz, $CDCl_3$) δ 8.73 (s, 1H), 8.29 (d, *J* = 8.1 Hz, 1H), 8.19 (brt, 1H), 8.04 (dt, *J* = 8.1, 1.8 Hz 1H), 7.48 (td, *J* = 7.6, 1.8 Hz, 1H), 7.45-7.42 (m, 1H), 7.30-7.29 (m, 2H), 7.25-7.23 (m, 2H), 7.12-7.07 (m, 2H), 3.78 (q, *J* = 7.0 Hz, 2H), 3.04 (t, *J* = 7.0 Hz, 2H); ^{13}C NMR (151 MHz, $CDCl_3$) δ 163.55, 160.61, 159.04, 148.15, 147.41, 136.82, 133.48, 130.49, 129.92, 129.84, 127.68, 125.23, 124.29, 124.20, 123.56, 121.28, 115.82, 114.76, 38.93, 28.76; ESI-HRMS (*m/z*) calcd $C_{20}H_{16}F_2N_2O$ (M + H^+) 339.1303; found 339.1309.

***N*-(2-Fluorophenethyl)-5-(3-fluorophenyl)picolinamid (30h).** White solid, yield 65%. ^{1}H NMR (600 MHz, $CDCl_3$) δ 8.72 (d, *J* = 2.2 Hz, 1H), 8.26 (d, *J* = 8.1 Hz, 1H), 8.17 (brs, 1H), 8.00 (dd, *J* = 8.1, 2.2 Hz, 1H), 7.49-7.45 (m, 1H), 7.39 (d, *J* = 7.7 Hz, 1H), 7.30 (dd, *J* = 8.0, 1.6 Hz, 1H), 7.26-7.21 (m, 2H), 7.14-7.10 (m, 1H),

7.08-7.04 (m, 2H), 3.76 (q, J = 7.1 Hz, 2H), 3.02 (t, J = 7.1 Hz, 2H); ^{13}C NMR (151 MHz, $CDCl_3$) δ 163.67, 162.81, 160.73, 148.26, 145.98, 138.53, 137.25, 135.02, 130.51, 130.24, 127.76, 125.12, 123.61, 122.34, 121.67, 115.00, 114.79, 113.61, 39.03, 28.71; ESI-HRMS (*m/z*) calcd $C_{20}H_{16}F_2N_2O$ (M + H^+) 339.1303; found 339.1306.

***N*-(2-Fluorophenethyl)-5-(4-fluorophenyl)picolinamide (30i).** White solid, yield 69%. ^{1}H NMR (600 MHz, $CDCl_3$) δ 8.70 (d, J = 2.2 Hz, 1H), 8.25 (d, J = 8.1 Hz, 1H), 8.14 (brs, 1H), 7.97 (dd, J = 8.1, 2.2 Hz, 1H), 7.59-7.56 (m, 2H), 7.25-7.23 (m, 1H), 7.21-7.18 (m, 3H), 7.09-7.03 (m, 2H), 3.76 (q, J = 7.0 Hz, 2H), 3.02 (t, J = 7.0 Hz, 2H); ^{13}C NMR (151 MHz, $CDCl_3$) δ 163.58, 162.44, 160.39, 147.98, 145.81, 137.44, 134.73, 132.55, 130.49, 128.36, 127.69, 125.22, 123.56, 121.60, 115.65, 114.76, 38.94, 28.75; ESI-HRMS (*m/z*) calcd $C_{20}H_{16}F_2N_2O$ (M + H^+) 339.1303; found 339.1304.

***N*-(2-Fluorophenethyl)-5-(2-hydroxyphenyl)picolinamide (30j).** White solid, yield 70%. ^{1}H NMR (600 MHz, DMSO-d_6) δ 9.82 (s, 1H), 8.83 (t, J = 7.0 Hz, 1H), 8.80 (d, J = 2.0 Hz, 1H), 8.14 (dd, J = 8.1, 2.0 Hz, 1H), 8.05 (d, J = 8.1 Hz, 1H), 7.38 (d, J = 7.6 Hz, 1H), 7.33 (t, J = 7.6 Hz, 1H), 7.27-7.25 (m, 2H), 7.16-7.12 (m, 2H), 7.01 (d, J = 8.1 Hz, 1H), 6.95 (t, J = 7.6 Hz, 1H), 3.59 (q, J = 7.0 Hz, 2H), 2.94 (t, J = 7.0 Hz, 2H) ^{13}C NMR (151 MHz, DMSO-d_6) δ 163.64, 160.26, 154.50, 148.10, 147.74, 137.40, 136.51, 130.96, 130.16, 129.73, 128.09, 125.83, 124.16, 123.42, 121.07, 119.60, 116.09, 114.93, 38.85, 28.36; ESI-HRMS (*m/z*) calcd $C_{20}H_{17}FN_2O_2$ (M + H^+) 337.1347; found 337.1348.

***N*-(2-Fluorophenethyl)-5-(3-hydroxyphenyl)picolinamide (30k).** White solid, yield 66%. ^{1}H NMR (600 MHz, DMSO-d_6) δ 9.72 (s, 1H), 8.93 (t, J = 7.0 Hz, 1H), 8.86 (d, J = 2.0 Hz, 1H), 8.19 (dd, J = 8.1, 2.0 Hz, 1H), 8.07 (d, J = 8.1 Hz, 1H), 7.63-7.61 (m, 1H), 7.34 (t, J = 7.8 Hz, 2H), 7.33-7.32 (m, 1H), 7.20-7.19 (m, 1H), 7.15-7.11 (m, 2H), 6.89-6.87 (m, 1H), 3.58 (q, J = 7.0 Hz, 2H), 2.93 (t, J = 7.0 Hz, 2H); ^{13}C NMR (151 MHz, DMSO-d_6) δ 163.50, 160.50, 157.90, 148.67, 146.14, 137.88, 137.43, 135.24, 130.95, 130.13, 128.51, 128.05, 124.17, 121.79, 117.69,

115.59, 114.93, 113.70, 38.88, 28.34; ESI-HRMS (*m/z*) calcd $C_{20}H_{17}FN_2O_2$ (M + H^+) 337.1347; found 337.1350.

***N*-(2-Fluorophenethyl)-5-(4-hydroxyphenyl)picolinamide (30l).** White solid, yield 65%. ^{1}H NMR (600 MHz, DMSO-d_6) δ 9.73 (s, 1H), 8.85 (d, *J* = 2.0 Hz, 1H), 8.79 (t, *J* = 7.0 Hz, 1H), 8.16 (dd, *J* = 8.2, 2.0 Hz, 1H), 8.03 (d, *J* = 8.2 Hz, 1H), 7.64 (d, *J* = 8.6 Hz, 2H), 7.34-7.31 (m, 1H), 7.27-7.26 (m, 1H), 7.16-7.11 (m, 2H), 6.92 (d, *J* = 8.6 Hz, 2H), 3.58 (q, *J* = 7.0 Hz, 2H), 2.93 (t, *J* = 7.0 Hz, 2H); ^{13}C NMR (151 MHz, DMSO-d_6) δ 163.60, 160.53, 158.14, 147.67, 145.51, 137.73, 134.18, 130.95, 128.17, 128.09, 126.61, 125.89, 124.16, 121.71, 115.94, 114.93, 38.85, 28.36; ESI-HRMS (*m/z*) calcd $C_{20}H_{17}FN_2O_2$ (M + H^+) 337.1347; found 337.1345.

***N*-(2-Fluorophenethyl)-5-(2-methoxyphenyl)picolinamide (30m).** White solid, yield 70%. ^{1}H NMR (600 MHz, $CDCl_3$) δ 8.68 (d, *J* = 2.1 Hz, 1H), 8.22 (d, *J* = 8.1 Hz, 1H), 8.18 (brs, 1H), 8.00 (dd, *J* = 8.1, 2.1 Hz, 1H), 7.41-7.38 (m, 1H), 7.33 (dd, *J* = 7.5, 1.5 Hz, 1H), 7.26-7.25 (m, 1H), 7.22-7.21 (m, 1H), 7.09-7.06 (m, 2H), 7.04-7.01 (m, 2H), 3.83 (s, 3H), 3.75 (q, *J* = 7.0 Hz, 2H), 3.01 (t, *J* = 7.0 Hz, 2H); ^{13}C NMR (151 MHz, $CDCl_3$) δ 164.45, 162.13, 156.60, 148.60, 147.97, 137.87, 136.81, 131.06, 130.58, 130.02, 128.18, 126.32, 125.96, 124.11, 121.48, 121.13, 115.40, 111.39, 55.52, 39.49, 29.39; ESI-HRMS (*m/z*) calcd $C_{21}H_{19}FN_2O_2$ (M + H^+) 351.1503; found 351.1508.

***N*-(2-Fluorophenethyl)-5-(3-methoxyphenyl)picolinamide (30n).** White solid, yield 65%. ^{1}H NMR (600 MHz, $CDCl_3$) δ 8.72 (s, 1H), 8.23 (d, *J* = 8.1 Hz, 1H), 8.16 (brs, 1H), 7.99 (d, *J* = 8.1 Hz, 1H), 7.41-7.38 (m, 1H), 7.26-7.24 (m, 1H), 7.22-7.20 (m, 1H), 7.19-7.16 (m, 1H), 7.11 (d, *J* = 1.8 Hz, 1H), 7.07 (t, *J* = 7.5 Hz, 1H), 7.05-7.02 (m, 1H), 6.97 (d, *J* = 7.5 Hz, 1H), 3.86 (d, *J* = 1.8 Hz, 3H), 3.75 (q, *J* = 7.2 Hz, 2H), 3.00 (t, *J* = 7.2 Hz, 2H); ^{13}C NMR (151 MHz, DMSO-d_6) δ 164.06, 161.22, 160.35, 149.33, 147.03, 138.17, 136.13, 131.62, 130.81, 128.76, 126.48, 124.82, 122.36, 119.87, 115.66, 115.52, 114.82, 113.08, 55.73, 39.51, 28.97. ESI-HRMS (*m/z*) calcd $C_{21}H_{19}FN_2O_2$ (M + H^+) 351.1503; found 351.1508.

***N*-(2-Fluorophenethyl)-5-(4-methoxyphenyl)picolinamide (30o).** White solid, yield 62%. ^{1}H NMR (600 MHz, $CDCl_3$) δ 8.73 (dd, *J* = 2.2, 0.6 Hz, 1H), 8.24 (dd, *J* =

8.1, 0.6 Hz, 1H), 8.17 (brs, 1H), 7.99 (dd, *J* = 8.1, 2.2 Hz, 1H), 7.58-7.57(m, 2H), 7.30-7.28(m, 1H), 7.26-7.22 (m, 1H), 7.11-7.07 (m, 2H), 7.06-7.04 (m, 2H), 3.89 (s, 3H), 3.78 (q, *J* = 7.0 Hz, 2H), 3.04 (t, *J* = 7.2 Hz, 2H); ^{13}C NMR (151 MHz, $CDCl_3$) δ 163.79, 160.74, 159.61, 147.32, 145.56, 138.02, 134.20, 130.50, 128.74, 127.75, 127.66, 125.27, 123.55, 121.55, 114.75, 114.09, 54.79, 38.91, 28.77; ESI-HRMS (*m/z*) calcd $C_{21}H_{19}FN_2O_2$ (M + H^+) 351.1503; found 351.1505.

5-(2-Cyanophenyl)-*N*-(2-fluorophenethyl)picolinamide (30p). White solid, yield 64%. ^{1}H NMR (600 MHz, $CDCl_3$) δ 8.59 (d, *J* = 2.2 Hz, 1H), 8.22 (d, *J* = 8.0 Hz, 1H), 8.16 (t, *J* = 7.0 Hz, 1H), 7.92 (dd, *J* = 8.0, 2.2 Hz, 1H), 7.70 (d, *J* = 7.6 Hz, 1H), 7.56 (td, *J* = 7.5, 1.2 Hz, 1H), 7.50 (td, *J* = 7.6, 1.0 Hz, 1H), 7.39 (d, *J* = 7.5 Hz, 1H), 7.26-7.25 (m, 1H), 7.22-7.20 (m, 1H), 7.09-7.07 (m, 1H), 7.06-7.02 (m, 1H), 3.74 (q, *J* = 7.0 Hz, 2H), 3.00 (t, *J* = 7.0 Hz, 2H); ^{13}C NMR (151 MHz, $CDCl_3$) δ 170.06, 163.52, 160.45, 148.31, 147.05, 137.78, 136.63, 135.16, 134.47, 130.48, 130.27, 129.98, 128.11, 127.87, 127.70, 125.18, 123.60, 121.25, 114.77, 38.93, 28.75; ESI-HRMS (*m/z*) calcd $C_{21}H_{16}FN_3O$ (M + H^+) 346.1350; found 346.1350.

5-(3-Cyanophenyl)-*N*-(2-fluorophenethyl)picolinamide (30q). White solid, yield 69%. ^{1}H NMR (600 MHz, $CDCl_3$) δ 8.75 (d, *J* = 2.0 Hz, 1H), 8.32 (d, *J* = 8.1 Hz, 1H), 8.17 (brs, 1H), 8.04 (dd, *J* = 8.1, 2.0 Hz, 1H), 7.91 (s, 1H), 7.86 (d, *J* = 7.8 Hz, 1H), 7.76 (d, *J* = 7.8 Hz, 1H), 7.66 (t, *J* = 7.8 Hz, 1H), 7.27-7.25 (m, 1H), 7.24-7.23 (m, 1H), 7.12-7.11 (m, 1H), 7.10-7.06 (m, 1H), 3.79 (q, *J* = 7.0 Hz, 2H), 3.04 (t, *J* = 7.0 Hz, 2H); ^{13}C NMR (151 MHz, $CDCl_3$) δ 163.25, 160.31, 148.96, 145.86, 137.79, 136.15, 135.08, 131.41, 130.93, 130.49, 130.14, 129.52, 127.75, 125.14, 123.58, 121.80, 117.65, 114.79, 112.99, 39.00, 28.73; ESI-HRMS (*m/z*) calcd $C_{21}H_{16}FN_3O$ (M + H^+) 346.1350; found 346.1350.

5-(4-Cyanophenyl)-*N*-(2-fluorophenethyl)picolinamide (30r). White solid, yield 61%. ^{1}H NMR (600 MHz, $CDCl_3$) δ 8.75 (d, *J* = 1.5 Hz, 1H), 8.30 (d, *J* = 8.1 Hz, 1H), 8.15 (brs, 1H), 8.04 (dd, *J* = 8.1, 1.5 Hz, 1H), 7.80 (d, *J* = 8.1 Hz, 2H), 7.72 (d, *J* = 8.1 Hz, 2H), 7.24-7.21 (m, 2H), 7.09 (t, *J* = 7.4 Hz, 1H), 7.05 (t, *J* = 8.0 Hz, 1H), 3.76 (q, *J* = 7.0 Hz, 2H), 3.02 (t, *J* = 7.0 Hz, 2H); ^{13}C NMR (151 MHz, $CDCl_3$) δ 163.23, 160.51, 149.09, 145.99, 140.88, 136.44, 135.19, 132.37, 130.48, 127.76,

127.31, 125.13, 123.60, 121.78, 117.77, 114.79, 111.88, 39.00, 28.72; ESI-HRMS (*m/z*) calcd $C_{21}H_{16}FN_3O$ (M + H^+) 346.1350; found 346.1352.

5.2 MTT cell viability assay

The cytotoxicity of synthesized compounds was measured by MTT assay. Briefly, LM3 cells were cultured in DMEM or RPMI-1640 medium supplemented with 10% FBS, 100 U/mL penicillin and 100 μg/mL streptomycin in a humidified incubator at 37 °C in an atmosphere of 5% CO_2. 5×10^3 Cells per well were seeded into 96-well plates and treated with tested compounds or DMSO (diluent) for 48h. Then the medium with compounds or DMSO was replaced with 180 μL fresh medium along with 20 μL MTT solution (5 mg/mL in PBS) per well and incubated at 37 °C for 4 h. Next, the MTT-containing medium was replaced with 150 μL of DMSO. After newly formed formazan crystals was dissolved, absorbance of each well was determined by a microplate reader (SpectraMax M4, Molecular Device) at a 570 nm wavelength. Assays were performed in triplicates. Growth inhibition rates were calculated with the following equation:

$$\text{Inhibition ratio } \% = \frac{\mathrm{OD_{DMSO}} - \mathrm{OD_{Compd}}}{\mathrm{OD_{DMSO}} - \mathrm{OD_{blank}}} \times 100\%$$

5.3 Dual Luciferase-Reporter Assay.

LM3 Cells were seeded into 24-well plate and co-transfected with luciferase reporter plasmid (pGL3-HRE-Luc) containing five copies of HREs and pRL-SV40 plasmid encoding Renilla luciferase using Lipofectamine 2000 transfection reagent (Invitrogen) according to the manufacturer's instructions, followed by incubation under normoxia (21% O_2) for 6h. Subsequently, the medium of each well was replace with fresh medium containing DMSO or tested compounds, and the plates were incubated under normoxia for 1 h as well as hypoxia (1% O_2) for another 24h. The cells were washed with PBS buffer, lysed and subjected to determine luciferase activity using dual-luciferase reporter assay kit (Promega) according to the manufacturer's instructions. Luminescence was measured using a microplate reader

(SpectraMax M4, Molecular Device). The firefly luminescence signals were normalized to the activities of Renilla luciferase. Results were obtained from three independent determinations and presented as mean ± SD.

5.4 Western blotting assay.

Western blots were conducted as described previously. Briefly, Cells were seeded in 60 mm dishes and cultured under normoxia condition. After 70-80% confluence, cells were treated with indicated concentrations of tested compounds or DMSO (diluent) under normoxia for 1h and hypoxia for another 24h. Subsequently, cells were harvest and lysed with RIPA lysis buffer. Cell extracts were separated by SDA-PAGE electrophoresis and transferred onto polyvinylidene fluoride (PVDF) membranes (Millipore). The membranes were then blocked with 10% non-fat milk in TBST (Tris-buffered saline (TBS) containing 0.1% Tween-20) and reacted with primary antibodies (Proteintech), followed by incubation with secondary antibodies conjugated with horseradish peroxidase (HRP, purchased from Cell Signaling Technology). The protein bands were developed by the chemiluminescent reagents (Millipore).

5.5 Real-time PCR assay.

HUVECs were treated with **30m** or DMSO (diluent) under normoxia for 1h and hypoxia for another 24 h. Total RNA was extracted using TRIzol reagent (Invitrogen) and reverse transcription was performed using primescript RT reagent kit (Takara) to obtain cDNA, which was subsequently amplified by Real-time PCR using SYBR Premix Ex Taq II (Takara). The gene expression was calculated by $2^{-\Delta\Delta Ct}$ method and normalized by GAPDH as an internal control. Results were obtained from three independent determinations and presented as mean ± SD.

5.6 Capillary-like tube formation assay.

Capillary-like tube formation assay was performed according to the procedure reported previously.[38] Briefly, 96-well plates were coated with matrigel (Corning) and

incubated at 37 °C for gelation. HUVECs (3×10^4 per well) mixed with tested compound or DMSO (diluent) were seeded to the top of gel and incubated under hypoxia for 12 hours. Capillary-like tube was observed and imaged with inverted microscope containing CCD camera (Olympus).

5.7 Zebrafish angiogenesis assay

The zebrafish angiogenesis studies and procedures were approved by the Animal Ethics Committee of School of Pharmacy, Fudan University. The transgenic zebrafish (fil1:EGFP) embryos at 48 hpf were incubated in 6-well plates (n=10 per well) with 2 mL aquaculture water **30m** (0.5 and 1 μM) or DMSO for 24 h. Apatinib (0.5 μM) was used as positive control. The effects of tested compounds on SIVs of zebrafish were observed every with a con-focal microscopy. The numbers of SIVs were counted under con-focal microscopy. Results were obtained from three independent determinations and presented as mean ± SD.

5.8 Wound healing assay.

Cells were seeded in six-well and cultured under normoxia until about 90% confluence. A single scratch wound was created on cellular monolayer using a sterile micropipette tip. Subsequently, cells were incubated with compound **30m** at indicated concentrations or DMSO (diluent) under normoxia for 1h and hypoxia for another 24h. Migrating cells was observed and imaged with inverted microscope containing CCD camera (Olympus).

5.9 Transwell assay.

2×10^5 Cells suspending in 0.3 mL serum-free medium per well were seeded into the upper chamber (Corning). For invasion assay, the chamber was pre-coated with matrigel to simulate basement membrane. The chamber was then placed into 24-well plates, and the lower wells was added complete medium containing 10% FBS and indicated concentrations of compound **30m** or DMSO (diluent). The plate was incubated under normoxia for 1h and hypoxia for another 24 h. Cells migrated across

the chamber were fixed with methanol, stained with crystal violet, and subsequently counted from 5 different areas per well under inverted microscope. Results were obtained from three independent determinations and presented as mean ± SD.

5.10 *In vivo* anti-metastatic assay

All animal studies and procedures were approved by the Animal Ethics Committee of School of Pharmacy, Fudan University. Female BALB/c nude mice at 4−5 weeks of age were purchased from Shanghai Slac Laboratory Animal Co. Ltd. (Shanghai, China) and housed in individual ventilated cages (IVC) under specific pathogen free environment in animal holding unit (AHU) of Fudan University (Shanghai, China). MDA-MB-231 cells (2×10^5 per mouse) stably expressing luciferase were injected intravenously via tail vein of nude mice. 24 hours after injection, mice were randomized into groups (n = 4) and treated intraperitoneally with 15 and 30 mg/kg compound **30m** (dissolved in PBS containing 5% ethanol and 5% cremophor EL, 0.2 mL per mouse) or vehicle control (0.2 mL diluent) once every 2 days during 20 days. Metastatic tumors were detected and quantified using bioluminescent imaging according to the literatures. After imagination, the mice were weighed and sacrificed, and their lung tissues were collected, fixed with 4% paraformaldehyde and embedded in paraffin. Histochemistry analysis was performed to determine the metastatic nodules by H&E staining.

ASSOCIATED CONTENT

Supporting Information

The synthesis of intermediates **13a-c**, **16a-e**, **25a-b**; ^{1}H-NMR, ^{13}C-NMR spectra and purity table of target compounds; elements analysis of representative compounds. Molecular formula strings and some data (CSV). The Supporting Information is available free of charge on the ACS Publications web site at DOI: XXXX.

AUTHOR INFORMATION

Corresponding authors

*E-mail: xhliuhx@163.com; Tel & Fax: +86-551-65172353 (X. L.).

*E-mail: wangyang@shmu.edu.cn; Tel: +86-21-51980115 (Y. W.).

Author Contributions

[#] M. L., Y. L., and Z. Z. are co-first authors and contributed equally to this work.

Notes

The authors declare no competing financial interest.

ACKNOWLEDGMENTS

This study was supported by grants from Natural Science Foundation of China (21572003 to X. L.; 21472025 and 21877015 to Y. W.; 81972040 to R. L.), by Opening Project of Shanghai Key Laboratory of New Drug Design (SKLNDD-KF-201704), by Natural Science Research Program of Anhui Educational Committee (KJ2019A0232) and by Scientific Research Grants of Anhui Medical University (XJ201627).

ABREVIATIONS

HIF, hypoxia-inducible factor; SAR, structure activity relationship; VEGF, vascular epidermal growth factor; VHL, von Hippel–Lindau; HRE, hypoxia responsive element; MMP, matrix metalloproteases; EMT, epithelial-mesenchymal transition; DMF, *N*,*N*-dimethylformamide; DIPEA, *N*,*N*-diisopropylethylamine; IRs, inhibition rates; HUVECs, human umbilical vein endothelial cells; GFP, green fluorescent protein; GLUT1, glucose transporter type 1; SIVs, subintestinal vessels; ECM, extracellular matrix; H&E staining, hematoxylin and eosin staining; SD, standard deviation; TLC, thin-layer chromatography; TMS, tetramethylsilane; HRMS, high-resolution mass spectrometry; NMR, nuclear magnetic resonance; ESI, electrospray ionization; FBS, fetal bovine serum; PBS, phosphate buffer saline; TBS, tris-buffered saline; PVDF, polyvinylidene fluoride; HRP, horseradish peroxidase; IVC, individual ventilated cages.

REFERENCES

(1) Lambert, A. W.; Pattabiraman, D. R.; Weinberg, R. A. Emerging Biological Principles of Metastasis. *Cell* **2017**, *168*, 670-691.

(2) Valastyan, S.; Weinberg, R. A. Tumor metastasis: molecular insights and evolving paradigms. *Cell* **2011**, *147*, 275-292.

(3) Wan, L.; Pantel, K.; Kang, Y. Tumor metastasis: moving new biological insights into the clinic. *Nat. Med.* **2013**, *19*, 1450-1464.

(4) Guan, X. Cancer metastases: challenges and opportunities. *Acta. Pharm. Sin. B* **2015**, *5*, 402-418.

(5) Wells, A.; Grahovac, J.; Wheeler, S.; Ma, B.; Lauffenburger, D. Targeting tumor cell motility as a strategy against invasion and metastasis. *Trends Pharmacol. Sci.* **2013**, *34*, 283-289.

(6) Sun, Y.; Ma, L. The emerging molecular machinery and therapeutic targets of metastasis. *Trends Pharmacol. Sci.* **2015**, *36*, 349-359.

(7) Bruick, R. K.; McKnight, S. L. A conserved family of prolyl-4-hydroxylases that modify HIF. *Science* **2001**, *294*, 1337−1340.

(8) Kamura, T.; Sato, S.; Iwai, K.; Czyzyk-Krzeska, M.; Conaway, R. C.; Conaway, J. W. Activation of HIF1alpha ubiquitination by a reconstituted von Hippel-Lindau (VHL) tumor suppressor complex. *Proc. Natl. Acad. Sci. U. S. A.* **2000**, *97* (19), 10430-10435.

(9) Semenza, G. L. Defining the role of hypoxia-inducible factor 1 in cancer biology and therapeutics. *Oncogene* **2010**, *29*, 625-634.

(10) Koyasu, S.; Kobayashi, M.; Goto, Y.; Hiraoka, M.; Harada, H. Regulatory mechanisms of hypoxia-inducible factor 1 activity: Two decades of knowledge. *Cancer Sci.* **2018**, *109*, 560-571.

(11) Forsythe, J. A.; Jiang, B. H.; Iyer, N. V.; Agani, F.; Leung, S. W.; Koos, R. D.; Semenza, G. L. Activation of vascular endothelial growth factor gene transcription by hypoxia-inducible factor 1. *Mol. Cell. Biol.* **1996**, *16*, 4604-4613.

(12) Gilkes, D. M.; Semenza, G. L. Role of hypoxia-inducible factors in breast cancer metastasis. *Future Oncol.* **2013**, *9*, 1623-1636.

(13) Zhang, Y.; Fan, N.; Yang, J. Expression and clinical significance of hypoxia-inducible factor 1alpha, Snail and E-cadherin in human ovarian cancer cell lines. *Mol. Med. Rep.* **2015**, *12*, 3393-3399.

(14) Yang, M. H.; Wu, M. Z.; Chiou, S. H.; Chen, P. M.; Chang, S. Y.; Liu, C. J.; Teng, S. C.; Wu, K. J. Direct regulation of TWIST by HIF-1alpha promotes metastasis. *Nat. Cell Biol.* **2008**, *10*, 295-305.

(15) Kilic, M.; Kasperczyk, H.; Fulda, S.; Debatin, K. M. Role of hypoxia inducible factor-1 alpha in modulation of apoptosis resistance. *Oncogene* **2007**, *26*, 2027-2038.

(16) Semenza, G. L. Hypoxia-inducible factors: mediators of cancer progression and targets for cancer therapy. *Trends Pharmacol. Sci.* **2012**, *33*, 207-214.

(17) Wigerup, C.; Pahlman, S.; Bexell, D. Therapeutic targeting of hypoxia and hypoxia-inducible factors in cancer. *Pharmacol. Ther.* **2016**, *164*, 152-169.

(18) Gao, T.; Li, J. Z.; Lu, Y.; Zhang, C. Y.; Li, Q.; Mao, J.; Li, L. H. The mechanism between epithelial mesenchymal transition in breast cancer and hypoxia microenvironment. *Biomed. Pharmacother.* **2016**, *80*, 393-405.

(19) Unwith, S.; Zhao, H.; Hennah, L.; Ma, D. The potential role of HIF on tumour progression and dissemination. *Int. J. Cancer.* **2015**, *136*, 2491-2503.

(20) Moon, E. J.; Brizel, D. M.; Chi, J. T.; Dewhirst, M. W. The potential role of intrinsic hypoxia markers as prognostic variables in cancer. *Antioxid. Redox Signal.* **2007**, *9*, 1237−1294.

(21) Chen, C.; Lou, T. Hypoxia inducible factors in hepatocellular carcinoma. *Oncotarget* **2017**, *8*, 46691-46703.

(22) Kim, B. W.; Cho, H.; Chung, J. Y.; Conway, C.; Ylaya, K.; Kim, J. H.; Hewitt, S. M. Prognostic assessment of hypoxia and metabolic markers in cervical cancer using automated digital image analysis of immunohistochemistry. *J. Transl. Med.* **2013**, *11*, 185.

(23) Xia, Y.; Choi, H. K.; Lee, K. Recent advances in hypoxia-inducible factor (HIF)-1 inhibitors. *Eur. J. Med. Chem.* **2012**, *49*, 24-40.

(24) Bhattarai, D.; Xu, X.; Lee, K. Hypoxia-inducible factor-1 (HIF-1) inhibitors from the last decade (2007 to 2016): A "structure-activity relationship" perspective.

Med. Res. Rev. **2018**, *38*, 1404-1442.

(25) Li, Z.; You, Q.; Zhang, X. Small-molecule modulators of the hypoxia-inducible factor pathway: development and therapeutic applications. *J. Med. Chem.* **2019**, *62*, 5725-5749.

(26) Lee, K.; Lee, J. H.; Boovanahalli, S. K.; Jin, Y.; Lee, M.; Jin, X.; Kim, J. H.; Hong, Y. S.; Lee, J. J. (Aryloxyacetylamino)benzoic acid analogues: a new class of hypoxia-inducible factor-1 inhibitors. *J. Med. Chem.* **2007**, *50*, 1675-1684.

(27) Naik, R.; Won, M.; Kim, B. K.; Xia, Y.; Choi, H. K.; Jin, G.; Jung, Y.; Kim, H. M.; Lee, K. Synthesis and structure-activity relationship of (*E*)-phenoxyacrylic amide derivatives as hypoxia-inducible factor (HIF) 1alpha inhibitors. *J. Med. Chem.* **2012**, *55*, 10564-10571.

(28) Shimizu, K.; Maruyama, M.; Yasui, Y.; Minegishi, H.; Ban, H. S.; Nakamura, H. Boron-containing phenoxyacetanilide derivatives as hypoxia-inducible factor (HIF)-1 inhibitors. *Bioorg. Med. Chem. Lett.* **2010**, *20*, 1453–1456.

(29) Kwon, D. Y.; Lee, H. E.; Weitzel, D. H.; Park, K.; Lee, S. H.; Lee, C. T.; Stephenson, T. N.; Park, H.; Fitzgerald, M. C.; Chi, J. T.; Mook, R. A., Jr.; Dewhirst, M. W.; Lee, Y. M.; Hong, J. Synthesis and biological evaluation of manassantin analogues for hypoxia-inducible factor 1alpha inhibition. *J. Med. Chem.* **2015**, *58*, 7659-7671.

(30) Kim, H. S.; Hong, M.; Lee, S. C.; Lee, H. Y.; Suh, Y. G.; Oh, D. C.; Seo, J. H.; Choi, H.; Kim, J. Y.; Kim, K. W.; Kim, J. H.; Kim, J.; Kim, Y. M.; Park, S. J.; Park, H. J.; Lee, J. Ring-truncated deguelin derivatives as potent hypoxia inducible factor-1 inhibitors. *Eur. J. Med. Chem.* **2015**, *104*, 157–164.

(31) An, H.; Lee, S.; Lee, J. M.; Jo, D. H.; Kim, J.; Jeong, Y. S.; Heo, M. J.; Cho, C. S.; Choi, H.; Seo, J. H.; Hwang, S.; Lim, J.; Kim, T.; Jun, H. O.; Sim, J.; Lim, C.; Hur, J.; Ahn, J.; Kim, H. S.; Seo, S. Y.; Na, Y.; Kim, S. H.; Lee, J.; Lee, J.; Chung, S. J.; Kim, Y. M.; Kim, K. W.; Kim, S. G.; Kim, J. H.; Suh, Y. G. Novel hypoxia-inducible factor 1α (HIF-1α) inhibitors for angiogenesis-related ocular diseases: discovery of a novel scaffold via ring-truncation strategy. *J. Med. Chem.* **2018**, *61*, 9266-9286.

(32) Mooring, S. R.; Jin, H.; Devi, N. S.; Jabbar, A. A.; Kaluz, S.; Liu, Y.; Van

Meir, E. G.; Wang, B. Design and synthesis of novel small-molecule inhibitors of the hypoxia inducible factor pathway. *J. Med. Chem.* **2011**, *54*, 8471-8489.

(33) Mun, J.; Jabbar, A. A.; Devi, N. S.; Yin, S.; Wang, Y.; Tan, C.; Culver, D.; Snyder, J. P.; Van Meir, E. G.; Goodman, M. M. Design and in vitro activities of *N*-alkyl-*N*-[(8-*R*-2,2-dimethyl-2*H*-chromen-6-yl)methyl]heteroarylsulfonamides, novel, small-molecule hypoxia inducible factor-1 pathway inhibitors and anticancer agents. *J. Med. Chem.* **2012**, *55*, 6738-6750.

(34) Zhao, S.; Zhang, X.; Wei, P.; Su, X.; Zhao, L.; Wu, M.; Hao, C.; Liu, C.; Zhao, D.; Cheng, M. Design, synthesis and evaluation of aromatic heterocyclic derivatives as potent antifungal agents. *Eur. J. Med. Chem.* **2017**, *137*, 96-107.

(35) Huguet, F.; Melet, A.; Alves de Sousa, R.; Lieutaud, A.; Chevalier, J.; Maigre, L.; Deschamps, P.; Tomas, A.; Leulliot, N.; Pages, J. M.; Artaud, I. Hydroxamic acids as potent inhibitors of Fe(II) and Mn(II) E. coli methionine aminopeptidase: biological activities and X-ray structures of oxazole hydroxamate-EcMetAP-Mn complexes. *ChemMedChem* **2012**, *7*, 1020-1030.

(36) Zhu, W.; Wang, W.; Xu, S.; Wang, J.; Tang, Q.; Wu, C.; Zhao, Y.; Zheng, P. Synthesis, and docking studies of phenylpyrimidine-carboxamide derivatives bearing 1*H*-pyrrolo[2,3-b]pyridine moiety as c-Met inhibitors. *Bioorg. Med. Chem.* **2016**, *24*, 1749-1756.

(37) Lee, K.; Kang, J. E.; Park, S. K.; Jin, Y.; Chung, K. S.; Kim, H. M.; Lee, K.; Kang, M. R.; Lee, M. K.; Song, K. B.; Yang, E. G.; Lee, J. J.; Won, M. LW6, a novel HIF-1 inhibitor, promotes proteasomal degradation of HIF-1alpha via upregulation of VHL in a colon cancer cell line. *Biochem. Pharmacol.* **2010**, *80*, 982-989.

(38) Zhou, P.; Liang, Y.; Zhang, H.; Jiang, H.; Feng, K.; Xu, P.; Wang, J.; Wang, X.; Ding, K.; Luo, C.; Liu, M.; Wang, Y. Design, synthesis, biological evaluation and cocrystal structures with tubulin of chiral beta-lactam bridged combretastatin A-4 analogues as potent antitumor agents. *Eur. J. Med. Chem.* **2018**, *144*, 817-842.

Graphic Abstract

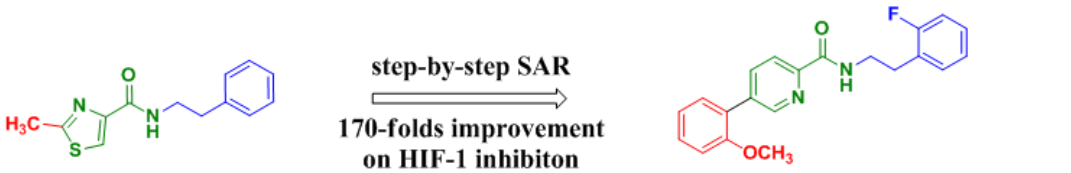

Preliminary hit **8**
$IC_{50} = 55.8$ μM
in HRE reporter assay

30m
$IC_{50} = 0.32$ μM
in HRE reporter assay
Potent anti-angiogenesis and anti-metastasis
in vitro and *in vivo*

Graphic Abstract

Discovery of Novel Aryl Carboxamide Derivatives as Hypoxia-inducible Factor (HIF) 1α Signaling Inhibitors with Potent Activities of Anticancer Metastasis

Mingming Liu[#], Yuru Liang[#], Zhongzhen Zhu[#], Jin Wang, Xingxing Cheng, Jiayi Cheng, Binpeng Xu, Rong Li, Xinhua Liu and Yang Wang**

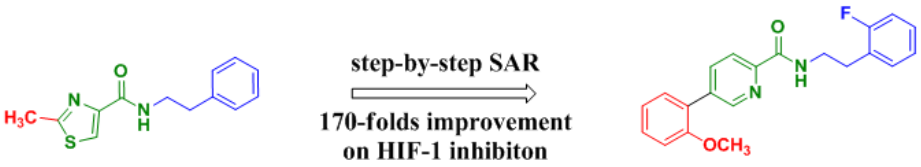

Preliminary hit **2**
IC_{50} = 55.8 μM
in HRE reporter assay

50m
IC_{50} = 0.32 μM
in HRE reporter assay
Potent anti-angiogenesis and anti-metastasis
in vitro and *in vivo*